sufficiently expressed. The amount of VA RNAs expressed from the chromosomes of the established cell lines may be insufficient, probably because abundant VA RNAs are necessary in the late phase of viral replication. Therefore, we adopted a strategy in which a VA-containing FG AdV (denoted pre-vector) is extensively amplified using 293 cells and the pre-vector is then converted to VA-deleted AdV through the removal of the VA genes using recombinase-expressing 293 cells to obtain a large amount of VA-deleted AdVs sufficient for the simultaneous introduction of numerous viral copies to the cells. However, this strategy appeared unrealizable because it requires the 293 cell line highly expressing the recombinase sufficient to remove VA RNA genes completely from rapidly replicating pre-vector genomes. We have established the 293 cell line, 293hde12[8], that contains the codon-humanized FLPe (hFLPe) that highly expresses thermo-stable FLPe recombinase[9]. We here showed that the VA genes present in the pre-vector genome were virtually completely removed using this cell line and high-titer VA-deleted AdVs were efficiently obtained.

Results

Efficient production of VA-deleted AdVs. We first constructed a VA-expressing DNA fragment, FVF, that contains intact VAI and VAII genes (Fig. 1a) flanked with a couple of FRTs (F refers to FRT in this study). The splicing acceptor site present between the initiation codon of the terminal protein precursor (pTP) and the 5′ end of VAI was disrupted by replacing T with C to prevent possible aberrant splicing. Then, we constructed two structurally different EF-AdV pre-vectors expressing GFP under the control of the EF1α promoter, AxdV-4FVF-GFP and AxdV-FVF-GFP, in which the original VAI and VAII genes were disrupted and, instead, the functional FVF fragment was inserted at different positions. The former pre-vector lacks both B-box sequences of the VAI and VAII that are essential for the activity of the internal polymerase-III promoter because of the deletions of 15 nt and 17 nt, respectively, (Fig. 1b), and instead bears the FVF fragment at the E4 insertion site near the right end of the viral genome[10] (Fig. 1a, upper left). The latter pre-vector lacks most of the VAI and VAII regions because of a deletion of 381 nt (Fig. 1c) and contains the FVF fragment within this region (Fig. 2a, lower left). Both pre-vectors grew well in the 293 cells, and their transduction titers were only slightly lower than that of the control FG AdV (Table 1, 37×10^7 and 60×10^7 versus 83×10^7 copies/mL).

Then, 293hde12 cells that constitutively and highly express codon-humanized FLPe recombinase[8,11] were infected with pre-vectors to obtain the first stock of VA-deleted AdV. The vector lacking VA RNA genes grew efficiently in the 293hde12 cells, similar to the pre-vector genome in 293 cells, because the VA RNAs were supplied from the excised circular DNAs consisting of VA RNA genes and one copy of FRT (Fig. 2a, middle) and from the pre-vector genome prior to the FLP-mediated excision. Then, five times more volume of the first stock than usual was used to infect the 293hde12 cells to create the second stock. The vector replicated in the 293hde12 cells, probably because a large amount of VA-deleted AdV were infected: the titer of the vector in the first stock was very high, and a much larger volume of stock was used for infection. The resulting vectors were named AxdV-4F-GFP and AxdV-F-GFP, respectively (Fig. 2a, upper and lower right). When the vectors in the second stock were used to infect 293hde12 cells, a minimal degree of replications was observed. Using a high multiplicity of infection (MOI), however, the slight replication was observed though the replication progressed slowly. Vectors from the second stock were used for further characterization.

The transduction titers of VA-deleted AdVs were sufficient for practical use. Because VA-deleted AdV is difficult to grow in 293 cells, the conventional titration method for measuring viral growth cannot be used. Therefore, the transduction titers[12] of the VA-deleted AdV and the pre-vector were measured; these titers show the copy number of viral genomes successfully transduced into infected target cells as evaluated using real-time PCR. The titers of VA-deleted AdV, pre-vector, and commonly used FG AdV can be compared using this method. The transduction titers of both AxdV-4F-GFP and AxdV-F-GFP were only one order lower than those of their pre-vectors (14% and 12%, respectively, Table 1), indicating that the titers of the VA-deleted vectors were sufficient for practical use as an alternative to FG AdVs. Moreover, using the same strategy, we produced other VA-deleted AdVs, such as AxdV-4F-NCre expressing Cre recombinase under the control of EF1α promoter and AxdV-F-SRChe expressing the Cherry marker under the control of the SRα promoter, and the resulting transduction titers were similar to those for AxdV-4F-GFP and AxdV-F-GFP (Table 1). Of note, the titer of Cre-expressing VA-deleted AdV was successfully obtained without trouble and was also quantitatively sufficient for general use, since Cre-expressing FG AdVs often exhibit a low titer and vector expansion is sometimes difficult.

Viral stocks of VA-deleted AdV likely contain a small amount of pre-virus that escaped the removal of the FVF fragment. Hence, HuH-7 cells were infected with AxdV-F-GFP and three days later, the transduced AdV DNA was examined using a Southern blot technique (Fig. 2b). The pre-vector DNA (2.7 kb) containing the VA genes clearly shifted to VA-deleted AdV DNA (2.2 kb), and no 2.7-kb band was detected in this assay. The result indicates that the VA RNAs in the pre-vector were efficiently removed during the replication of the pre-vector genome in 293hde12 cells. The same results were obtained when AxdV-4F-GFP was used (data not shown). The copy numbers of these viral genomes were examined using quantitative real-time PCR (qPCR) and VAI- and VAII-specific probes (Fig. 1a). Although the secondary structures of VAI and VAII are very similar, these probes were highly specific for one to the other (Supplementary Fig. S1). The pre-vector genome was present at approximately 1/90 or less, indicating that the purity of the VA-deleted AdV was about 99% or more.

Almost complete removal of contaminated pre-vector. To examine the level of VA RNAs expressed from contaminated pre-vector, the total cellular RNA of HuH-7 cells infected with AxdV-F-GFP was extracted and the expressed VA RNAs were analyzed using a northern blot technique (Fig. 2c). Neither VAI nor VAII were detected. In contrast, the pre-vector AxdV-FVF-GFP expressed considerable amounts of VAI and VAII. The same results were obtained when AxdV-4F-GFP was used (data not shown). The FG AdV AxCAGFP expressing GFP under control of CAG promoter does express similar amount of VA RNAs (data not shown). Expressed VAI and VAII RNA in cells infected with AxdV-4F-GFP or AxdV-F-GFP were also examined using qPCR after reverse transcription (Table 2). Both VAI and VAII were hardly detected, compared with the pre-vector infected in parallel, especially when using AxdV-4F-GFP, though 1% to 3% of the VA RNAs were detected when infected with AxdV-F-GFP. The Table 2 also showed that AxdV-4F-GFP and AxdV-F-GFP preparations expressed VA RNAI only about 1/300 and 1/120 less than FG AdV (0.02/5.97 and 0.05/5.97), respectively. These results correlated well with those of the Southern blot and qPCR analyses described above. Because contamination by the pre-vector of AxdV-4F-GFP was hardly detected using qPCR, an extremely sensitive bioassay was performed; 293 cells were infected with the VA-deleted AdV stock and the possible presences of pre-vector genome and VA RNAs expressed from the pre-vector were examined using Southern and northern blot techniques, respectively. Only the pre-vector genome must replicate efficiently in 293 cells. The amplified pre-vector genome was still not detected in a Southern blot analysis (Fig. 3a),

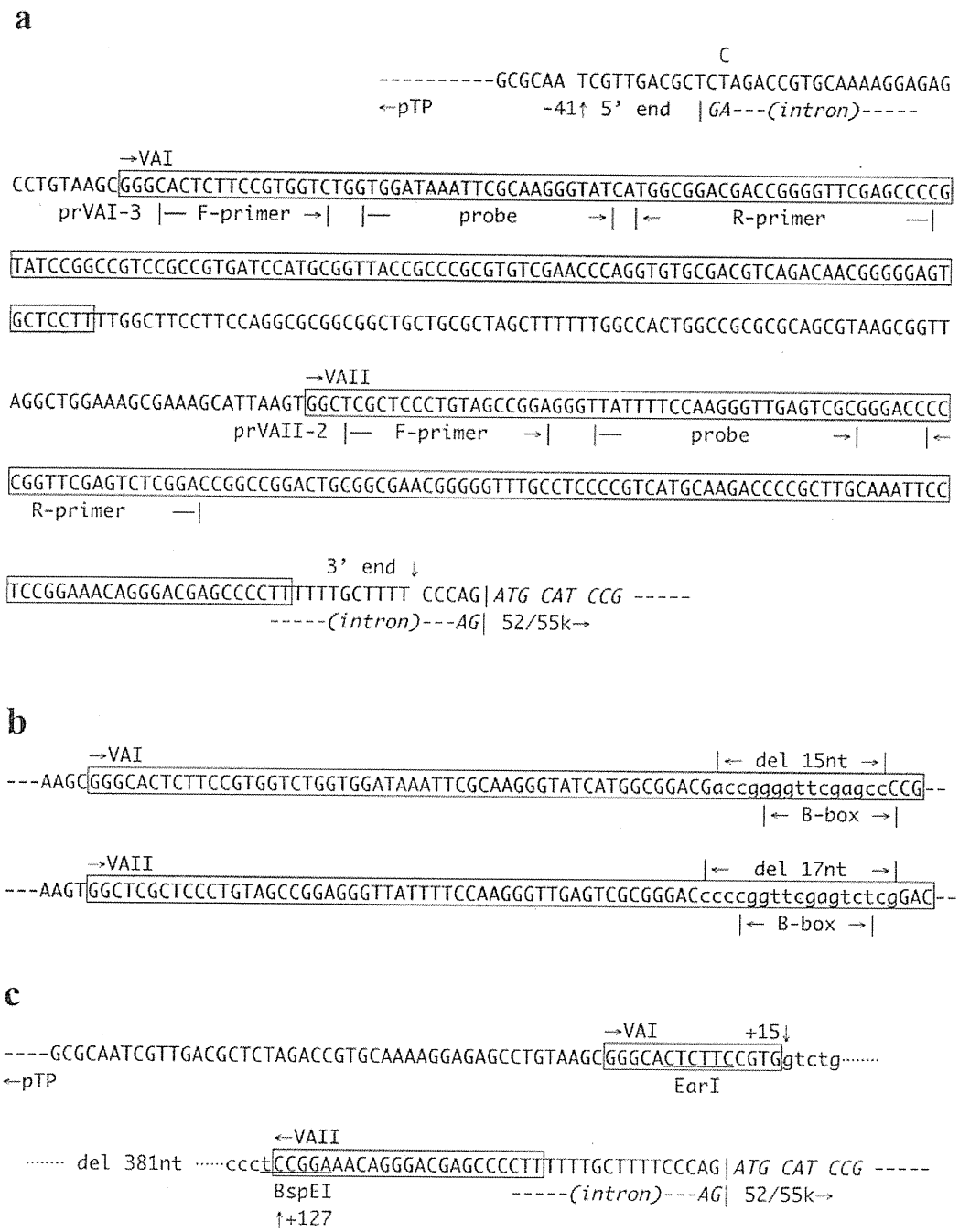

Figure 1 | Nucleotide sequences for VAI-VAII region. (a) VAI and VAII genes in the FVF fragment. VAI and VAII are boxed. prVAI-3 and prVAII-2 are the primers used for qPCR for the detection and quantification of VAI and VAII, respectively. Note that the actual R-primers are complementary to the sequences shown in this figure. pTP, terminal protein precursor; 52/55 k, 52 k and 55 k proteins. (b) B-box deletions of internal promoter in AxdV-4FVF-GFP and AxdV-4F-GFP. The deleted nucleotides are shown in small letters. (c) VAI-VAII deletion in AxdV-FVF-GFP and AxdV-F-GFP. The deleted region is shown in small letters. The deletion of 381 nt starts at 15 nt and 127 nt downstream from the 5' end of VAI and VAII, respectively.

whereas the VA RNAs were slightly detected using a northern blot technique (Fig. 3b). Although the experiments using 293 cells were not quantitative, these results suggested that the amount of VA RNAs expressed from contaminated pre-vector in target cells other than 293 cells was minimal when the second stock was used. These results indicated that the VA-deleted AdVs produced using this production system were almost pure and may be used without consideration of the effect of VA RNAs in most studies. The contaminated circular DNA containing the VA-RNA genes was completely removed by purification of the vector.

To examine whether the VA-deleted AdV expresses a gene product as efficiently as FG AdV, HeLa cells were infected with VA-deleted AdVs and pre-vectors expressing GFP at the same transduction unit value and the resulting fluorescence was measured (Table 3). The VA-deleted AdVs showed similar expression levels to those of their pre-vectors.

Discussion

The efficient removal of VA RNA genes from the pre-virus genomes is crucial for this strategy. We here showed that 293hde12 cell line

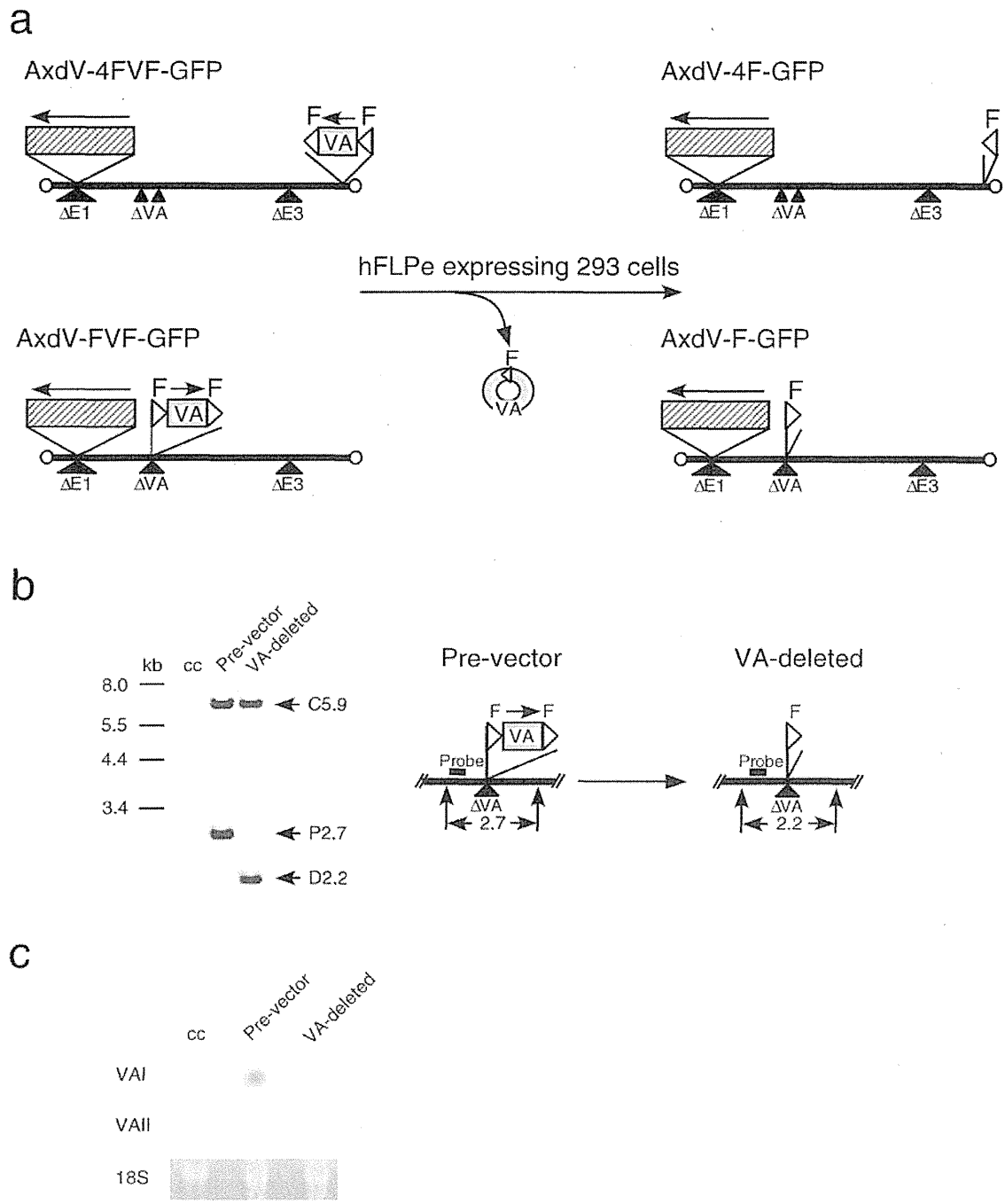

Figure 2 | Structures of pre-vectors and VA-deleted AdVs. (a) Strategy for the generation of VA-deleted vectors. F, FRT. Hatched box, GFP expression unit including EF1α promoter. An arrow shows the orientation of the transcription. (b) Removal of FVF fragment from the pre-vector AxdV-FVF-GFP genome. Total DNAs of infected HuH-7 cells were digested with *KpnI*, and the DNA fragment containing FVF and F was detected using a Southern blot technique using the probe shown in the figure (enzyme, positions). C5.9 refers to the 5.9-kb fragment derived from outside of this region (1.7-kb *BglII* fragment, nt 30823-82495), showing that the amounts of the vector genomes were almost the same. cc, uninfected control cells; P, pre-vector; D, VA-deleted AdV. (c) Detection of expressed VA RNAs. Total RNAs of the same infected HuH-7 cells were analyzed using a northern blot technique. 18 S, 18 S ribosomal RNA.

that highly and constitutively express FLP recombinase was sufficient for this purpose. The cell lines constitutively expressing Cre have been used for production of helper-dependent AdVs, which contain a large DNA up to about 30kb. The viral packaging region of the helper virus must be excised out from the replicating viral genome but the excision efficiency is less than that described here[13,14] and hence the contaminated helper virus must be removed by the buoyant centrifugation using cesium chloride. Probably such incomplete excision might result from the toxicity of highly expressed Cre in 293 cells[15–18], while no toxicity of FLP has so far been reported. Therefore, 293hde12 cells played the most important role in this production system.

Furthermore, we demonstrated in this work that the AdVs containing two FRT sequences at the VA RNA region in the viral

Table 1 | Transduction titers of VA-deleted AdVs

AdV	Type	Transduction titer copies/mL ($\times 10^7$)	Ratio (%)
AxdV-4FVF-GFP	pre-vector	37	100
AxdV-4F-GFP	VA-deleted	5	14
AxdV-FVF-GFP	pre-vector	60	100
AxdV-F-GFP	VA-deleted	7	12
AxdV-4FVF-NCre	pre-vector	47	100
AxdV-4F-NCre	VA-deleted	4	8
AxdV-FVF-SRChe	pre-vector	20	100
AxdV-F-SRChe	VA-deleted	2	12

The transduction titer of the control FG AdV, AxEFGFP, was 83×10^7 copies/mL. The transduction titer was called the relative vector titer (rVT)[12], which is about five-times lower than the conventional $TCID_{50}$ titer of the pre-virus measured using 293 cells (see Methods).

genome, AxdV-F-GFP etc., were viable and their titers were comparable to FG AdV. When a foreign DNA sequence is inserted into the AdV genome, even when the sequence is short such as recombination targets, the AdVs are often not viable or their titers are very low, probably because the small insertion influences on the replication of the AdV genome. For this reason only three positions, i.e. as the substitutions of E1 and E3 genes and the insertion upstream of E4 genes, are generally used. Hence, we first constructed AxdV-4F-GFP because we knew that the AdVs containing foreign DNA at the E4 insertion position was very stable shown by our early works[1,19]. Then, we tried the original site of VA RNA genes and demonstrated that the FRTs can successfully be inserted at the VA RNA region causing only slight reduction of the AdV titers.

This production system described here may allow the practical application of VA-deleted AdVs as a possible alternative to current FG AdVs, since the transduction titer was only one order lower than that of FG AdVs and, in fact, we have already produced more than twenty VA-deleted AdVs expressing various genes without any difficulty. Because VA RNAs may disturb experimental results that are obtained using FG AdVs to some extent, VA-deleted AdVs are likely to be preferable for many types of basic research using adenovirus vectors. When examining the influences of VA RNAs on previously obtained results, the pre-vector can be used as an ideal control for VA-deleted AdVs. Although the target genes of VA RNAs are not clear at present, Aparicio *et al.*[5] reported that the expressions of many genes including TIA-1, a splicing and translation regulator, are downregulated by mivaRNAs, which are the processed products of VA RNAs, and they proposed that TIA-1 may be one such target of mivaRNAs. We compared the expression of TIA-1 using a VA-deleted AdV and its pre-vector and observed that TIA-1 expression was slightly downregulated but was not statistically significant in our assay system. Because they did not use a VA-deleted vector but rather E1-containing viruses that efficiently replicate in infected cells and probably express much more VA RNAs. Therefore, their results are not necessarily contradictory and may be explained by the quantitative differences of expressed VA RNAs. We found other genes that were downregulated by VA RNAs (YK, unpublished results). Studies on the influences of VA RNAs on immune responses *in vivo* are also underway. So far, we found that the immune response caused by VA RNA was lower than that by aberrantly expressed viral pIX protein[20] but quantitative analyses are needed to clarify this issue. Notably, VA-deleted AdVs are probably superior to the current FG AdV for researches involving AdVs expressing siRNA and miRNA, since VA RNAs expressed by FG AdVs may compete with them and disturb the effects of these RNAs[3]. In fact, an shRNA expressed using VA-deleted AdV was more effective than that using current FG AdV (manuscript in preparation). These small-RNA technologies are extensively used in various research fields including signal transduction, cell differentiation and iPS study. Because more than three hundred papers have been published so far using FG AdVs expressing siRNA or miRNA based on our PubMed searching, VA-deleted AdV may be valuable in these fields.

The production level may be sufficient to apply VA-deleted AdVs to gene therapy as a safer alternative to existing practices. To what extent VA-deleted AdVs reduce immune responses in gene therapy of humans remain to be elucidated. Another possible contribution to gene therapy using AdVs is that, VA-deleted AdVs may considerably reduce contamination with replication-competent AdVs (RCA), one of the problems in the production of gene-therapy grade AdVs, because even if VA-deleted RCA is generated, only very low levels of replication would occur in human cells. Moreover, as proposed by Carnero *et al.*[4], a VA-deleted replication-competent adenovirus produced using this method could be used as an oncolytic virus that specifically replicate in cells with inactive PKR, such as tumor cells with activated ras or Epstein-Barr virus.

The same strategy described here could also be applied to studies of other DNA viruses, such as herpes viruses, because drug-resistant cell lines that highly express viral genes essential for the viral life cycle are often difficult to obtain because of their slight toxicity to cell growth. Moreover, using this strategy and recombinase-expressing cells, two or more genes could be deleted simultaneously using mutant *lox*P 2272[21] and FRT mutants[22,23] that exclusively recombine two identical mutant recombinase-targets. In conclusion, this strategy may accelerate studies using adenovirus vectors and may contribute to gene therapy.

Methods

Cells and virus titration. Human cell lines of 293[24], HeLa and HuH-7 are derived from the embryonic kidney, the cervical carcinoma and the hepatocellular carcinoma, respectively. These cells were cultured in DMEM supplemented with 10% fetal calf serum (FCS). The 293 cells constitutively express adenoviral E1 genes and support the replication of E1-substituted AdVs. 293hde12 is a 293 cell line possessing the hFLPe gene[8], an improved version of the FLPe gene[9], in which the codon usage has been changed to that used in humans and which produces more FLPe enzyme. 293hde12 cells were cultured in DMEM supplemented with 10% FCS plus geneticin (0.75 mg/mL). After infection with AdVs, the cells were maintained in DMEM supplemented with 5% FCS without geneticin.

All the AdVs were titrated using the method of transduction titer known as the relative vector titer (copies/mL)[12]. In this titration method, the copy number of viral genomes successfully transduced into the infected target cells, such as HeLa or HuH-7 cells, are measured using real-time PCR. The transduction titer method can be used not only for VA-deleted AdV, but also for FG AdVs, including the pre-vectors. This method enabled us to compare the various titers, since the transduction titer is not influenced by the growth rate of 293 cells, even if an expressed gene product (such as Cre or dsRed) is slightly deleterious to 293 cells[12]. When the gene product is not deleterious, the titer obtained using this method corresponds to about one fifth of that using either a 50% tissue culture infectious dose ($TCID_{50}$/mL)[25,26] or a plaque assay; the reason for this difference is probably because the transduction efficiency of 293 cells is much higher than that of other cells. The sequences of TaqMan probes for the titration (named AdV-1[19,12]) are derived from Ad5 pIX gene: forward primer, 5′-TGTGATGGGCTCCAGCATT-3′; probe, 5′-ATGGTCGCCCCGTCCTGCC-3′; reverse primer, 5′-TCGTAGGTCAAGGTAGTAGAGTTTGC-3′. A recommended protocol of the titration is available as Supplementary data of reference 12.

Table 2 | Expression levels of VAI and VAII RNAs measured using qPCR

		VA RNAs			
		I		II	
AdVs	Type	Copies $\times 10^8$	Ratio (%)	Copies $\times 10^8$	Ratio (%)
AxdV-4FVF-GFP	pre-vector	4.47 ± 0.81	100	1.36 ± 0.15	100
AxdV-4F-GFP	VA-deleted	0.02 ± 0.00	<1	ND	<1
AxdV-FVF-GFP	pre-vector	1.81 ± 0.06	100	1.83 ± 0.32	100
AxdV-F-GFP	VA-deleted	0.05 ± 0.00	2.9	0.03 ± 0.00	1.4
AxCAGFP	control FG AdV	5.97 ± 0.83		4.17 ± 0.16	

HuH-7 cells were infected with 50 μL of conventional stock of the pre-vector and the second stock of VA-deleted AdV. The method for preparation of the second stock is described in the Method section.

Plasmids. The pVA41da plasmid contains a DNA fragment covering the entire VAI and VAII from nt position 10576–11034 (Fig. 1a) of adenovirus type 5. A splicing acceptor site upstream of the pTp gene was disrupted, as described in the text. The region of functional VAI and VAII was excised as a *Hin*dIII-*Xba*I fragment and inserted at a *Swa*I site of pUFwF[27]; the resulting plasmid and DNA fragment containing intact VAI and VAII flanked two FRTs were named pUFVA41daF and FVF fragment, respectively.

Vector construction. All the AdVs described here were constructed using the cosmid cassette pAxcwit2 containing the full-length AdV genome[28]. The pre-vector cassette pAxdV-4FVF-w (w refers to the SwaI cloning site at the E1 region, see below) possesses the AdV genome in which VAI and VAII genes are disrupted by 15-nt and 17-nt deletions in their B-box sequences, respectively (Fig. 1b). The AdV genome contains the FVF fragment at the *Sna*BI site (nt position 35770) located in the E4 region at 165-nt downstream from the right end of the Ad5 genome[19]. A GFP-expressing unit under the control of the EF1α promoter[29] was inserted into the *Swa*I cloning site at the authentic E1 substitution region to obtain the pre-vector cosmid pAxdV-4FVF-GFP. The EF1α promoter in the left orientation was adopted to express the GFP because the use of the promoter in this manner greatly reduces the immune response of AdV, compared with the CAG and CMV promoters[20,30]. The pre-vector AxdV-4FVF-NCre and VA-deleted AdV AxdV-4F-NCre possess identical structures to AxdV-4FVF-GFP and AxdV-4F-GFP, respectively, except that the GFP gene is replaced by a Cre recombinase gene tagged with a nuclear localization signal[31]. The other pre-vector cosmid cassette pAxdV-FVF-4c lacks the VAI and VAII genes because of a large deletion from nt 10635 to nt 11012 and instead carries the FVF fragment. Note that this cassette contains two cloning sites, the *Swa*I site in the E1 region and the *Cla*I site in the E4 region (as described above), and is useful for the simultaneous expression of two genes. The pre-vector cosmid pAxdV-FVF-GFP was obtained by inserting the GFP expression unit described above at the *Swa*I site. Also, another pre-vector cosmid pAxdV-FVF-4Che contains the Cherry marker gene (Clontech) under the control of an SRα promoter[32] at this *Cla*I site. Then, the pre-vector AxdV-FVF-GFP, the VA-deleted vector AxdV-F-GFP, the pre-vector AxdV-FVF-4SRChe, and the VA-deleted AdV, AxdV-F-4SRChe were obtained using these pre-vector cosmid cassettes. The procedure to produce VA-deleted AdVs was as follows: the pre-vector genome in the cosmid cassette described above was excised with *Pac*I and transfected into 293 cells. The obtained pre-vector was then amplified twice using 293 cells and was used to infect 293hde12 cells at 10 copies/cell of transduction multiplicity of infection (MOI) to obtain VA-deleted AdVs. Then, This VA-deleted AdVs were used to infect 293hde12 cells at 10 copies/cell. The resultant viral stock is called the second stock in the Result section.

Quantitative Real-time PCR. The RNA expressions of VAI and VAII were quantified using the primers and probes described in Fig. 1a. The sequences of the GFP primers were as follows:
forward primer, CTACAACAGCCACAACGTCTATATCA;
probe, CGACAAGCAGAAGAACGGCATCAAGG;
reverse primer, ATGTTGTTGCGGATCTTGAAG.
The total RNA of the infected cells was extracted, and the amounts of the expressed

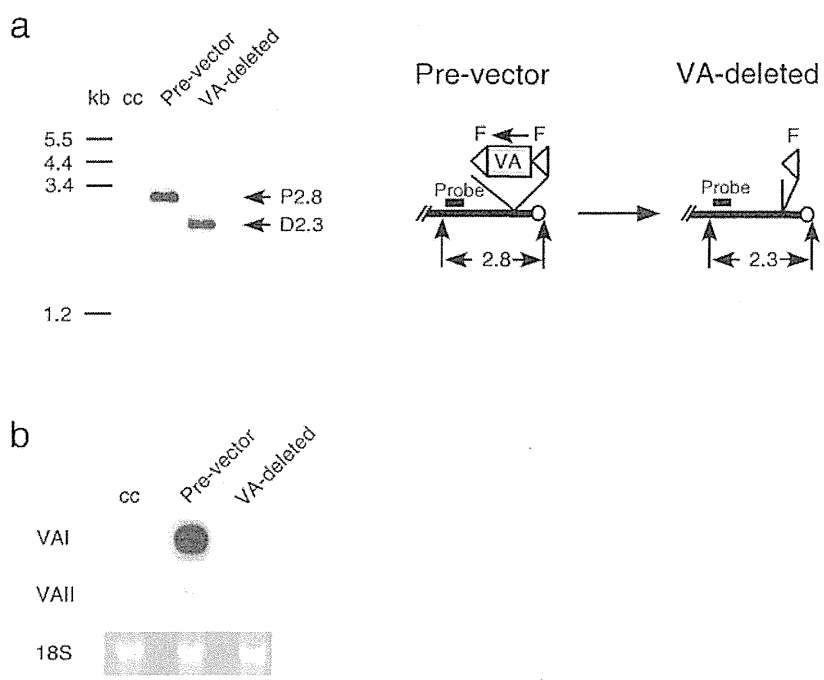

Figure 3 | Viral genome and expressed VA-RNA of contaminated pre-vector replicating in 293 cells. (a) Removal of the FVF fragment from the genome of the replicating pre-vector. Total DNAs of 293 cells infected with 15 μL of AxdV-4F-GFP stock were digested with *Eco*RV and the DNA fragment containing FVF and F was detected using a Southern blot technique. Other presentations are the same as in Fig. 1. (b) Detection of the expressed VA RNAs. Total RNAs of the same infected 293 cells were analyzed using a northern blot technique. 18 S, 18 S ribosomal RNA.

Table 3 | GFP expression in target cells infected with VA-deleted AdVs

AdV	Type	Ratio	
		fluorescence	expressed mRNA
AxdV-4FVF-GFP	pre-vector	1	1
AxdV-4F-GFP	VA-deleted	0.97 ± 0.15	0.81 ± 0.16
AxdV-FVF-GFP	pre-vector	1	1
AxdV-F-GFP	VA-deleted	1.14 ± 0.31	1.18 ± 0.20

HeLa cells were infected with pre-vector and VA-deleted AdV at a transduction MOI of 10. Three days later, GFP fluorescence was measured using a fluorometer and the GFP mRNA was quantified using reverse transcriptase and qPCR.

target RNA and 18S-rRNA (correction standard) were quantified using reverse-transcription and real-time PCR (Applied Biosystems Prism 7000); the ratio of the target RNA to 18S-rRNA was then calculated. The linear correlation between the amount of infected vector and the Ct values was confirmed (Supplementary Fig. S2). To quantify the DNA amount of VA RNAs and the AdV genome, the infected total cell DNA was prepared from cells using a previously described method[23,24] or a DNA preparation kit (Macherey-Nagel, through TaKaRa Bio). Quantitative PCR was performed to detect the AdV genome using a probe for the pIX gene described above[10,12]. The amount of chromosomal DNA was simultaneously measured to correct the Ct values of the viral genome per cell, and the corrected Ct was shown throughout. The probes were derived from the sequence of the human β-actin gene for HeLa and HuH7[10]. The qPCR reaction was performed according to the manufacturer's protocol: 50°C for 2 min and 95°C for 10 min, followed by 40 cycles of 95°C for 15 sec and 60°C for 1 min (Applied BioSystems).

Southern blotting analysis. HuH-7 cells in a 6-cm dish were infected with VA-deleted AdV and its pre-vector, and three days later the total DNA was prepared from the dish. Before alkaline treatment, the agarose gel was exposed to 0.1-N HCl for partial depurination, causing the DNA fragmentation of several hundred base pairs to obtain the complete transfer to the membrane[33]. The DNA was then transferred to the nylon membrane Hybond-N (Amersham GE) using the capillary-transfer method. Specific DNA was detected using a DIG DNA Labeling and Detection Kit (Roche Diagnostics). The probe DNA fragment derived from the viral genome was labeled with digoxigenin-UTP, and specific DNA was detected using the chemiluminescence of CDP-Star (Roche Diagnostics); the bands were visualized using LAS-4000 (Fuji Film).

Northern blotting analysis. The cells indicated in the figure legends were infected with pre-vector and VA-deleted AdV, respectively, at a transduction MOI of 10 copies/mL. The total RNA of the infected cells was extracted, and 30 μg per lane was electrophoresed in the agarose gel with tris-acetate-EDTA buffer. The RNA was transferred to the nylon membrane Hybond-N$^+$ (Amersham GE) using the capillary-transfer method. Specific RNA was detected using a DIGDNA Labeling and Detection Kit (Roche Diagnostics).

1. Miyake, S. *et al.* Efficient generation of recombinant adenoviruses using adenovirus DNA-terminal protein complex and a cosmid bearing the full-length virus genome. *Proc. Natl. Acad. Sci. U S A* **93**, 1320–1324 (1996).
2. Anton, M. & Graham, F. L. Site-specific recombination mediated by an adenovirus vector expressing the Cre recombinase protein: a molecular switch for control of gene expression. *J. Virol.* **69**, 4600–4606 (1995).
3. Lu, S. & Cullen, B. R. Adenovirus VA1 noncoding RNA can inhibit small interfering RNA and MicroRNA biogenesis. *J. Virol.* **78**, 12868–12876 (2004).
4. Carnero, E., Sutherland, J. D. & Fortes, P. Adenovirus and miRNAs. *Biochim. Biophys. Acta* **1809**, 660–667 (2011).
5. Aparicio, O. *et al.* Adenovirus VA RNA-derived miRNAs target cellular genes involved in cell growth, gene expression and DNA repair. *Nucleic Acids Res* **38**, 750–763 (2010).
6. Bhat, R. A., Domer, P. H. & Thimmappaya, B. Structural requirements of adenovirus VAI RNA for its translation enhancement function. *Mol. Cell Biol.* **5**, 187–196 (1985).
7. Machitani, M. *et al.* Development of an adenovirus vector lacking the expression of virus-associated RNAs. *J. Control Release* **154**, 285–289 (2011).
8. Takata, Y., Kondo, S., Goda, N., Kanegae, Y. & Saito, I. Comparison of efficiency between FLPe and Cre for recombinase-mediated cassette exchange in vitro and in adenovirus vector production. *Genes Cells* **16**, 765–777 (2011).
9. Buchholz, F., Angrand, P. O. & Stewart, A. F. Improved properties of FLP recombinase evolved by cycling mutagenesis. *Nat. Biotechnol.* **16**, 657–662 (1998).
10. Kanegae, Y. *et al.* High-level expression by tissue/cancer-specific promoter with strict specificity using a single-adenoviral vector. *Nucleic Acids Res.* **39**, e7 (2011).
11. Kondo, S., Takata, Y., Nakano, M., Saito, I. & Kanegae, Y. Activities of various FLP recombinases expressed by adenovirus vectors in mammalian cells. *J. Mol. Biol.* **390**, 221–230 (2009).
12. Pei, Z., Kondo, S., Kanegae, Y. & Saito, I. Copy number of adenoviral vector genome transduced into target cells can be measured using quantitative PCR: application to vector titration. *Biochem. Biophys. Res. Commun.* **417**, 945–950 (2012).
13. Ng, P., Evelegh, C., Cummings, D. & Graham, F. L. Cre levels limit packaging signal excision efficiency in the Cre/loxP helper-dependent adenoviral vector system. *J. Virol.* **76**, 4181–4189 (2002).
14. Ng, P., Parks, R. J. & Graham, F. L. Preparation of helper-dependent adenoviral vectors. *Methods Mol. Med.* **69**, 371–388 (2002).
15. Loonstra, A. *et al.* Growth inhibition and DNA damage induced by Cre recombinase in mammalian cells. *Proc. Natl. Acad. Sci. U S A* **98**, 9209–9214 (2001).
16. Pfeifer, A., Brandon, E. P., Kootstra, N., Gage, F. H. & Verma, I. M. Delivery of the Cre recombinase by a self-deleting lentiviral vector: efficient gene targeting in vivo. *Proc. Natl. Acad. Sci. U S A* **98**, 11450–11455 (2001).
17. Silver, D. P. & Livingston, D. M. Self-excising retroviral vectors encoding the Cre recombinase overcome Cre-mediated cellular toxicity. *Mol. Cell* **8**, 233–243 (2001).
18. Baba, Y., Nakano, M., Yamada, Y., Saito, I. & Kanegae, Y. Practical range of effective dose for Cre recombinase-expressing recombinant adenovirus without cell toxicity in mammalian cells. *Microbiol. Immunol.* **49**, 559–570 (2005).
19. Saito, I., Oya, Y., Yamamoto, K., Yuasa, T. & Shimojo, H. Construction of nondefective adenovirus type 5 bearing a 2.8-kilobase hepatitis B virus DNA near the right end of its genome. *J. Virol.* **54**, 711–719 (1985).
20. Nakai, M. *et al.* Expression of pIX gene induced by transgene promoter: possible cause of host immune response in first-generation adenoviral vectors. *Hum. Gene Ther.* **18**, 925–936 (2007).
21. Lee, G. & Saito, I. Role of nucleotide sequences of loxP spacer region in Cre-mediated recombination. *Gene* **216**, 55–65 (1998).
22. Schlake, T. & Bode, J. Use of mutated FLP recognition target (FRT) sites for the exchange of expression cassettes at defined chromosomal loci. *Biochemistry* **33**, 12746–12751 (1994).
23. Nakano, M., Ishimura, M., Chiba, J., Kanegae, Y. & Saito, I. DNA substrates influence the recombination efficiency mediated by FLP recombinase expressed in mammalian cells. *Microbiol. Immunol.* **45**, 657–665 (2001).
24. Graham, F. L., Smiley, J., Russell, W. C. & Nairn, R. Characteristics of a human cell line transformed by DNA from human adenovirus type 5. *J. Gen. Virol.* **36**, 59–74 (1977).
25. Precious, B. & Russell, W. C. Growth, purification and titration of adenoviruses. In *Virology: a practical approach.* (ed. Mahy, B. W. J.) 128–152 (IRL press, Oxford; 1991).
26. Kanegae, Y., Makimura, M. & Saito, I. A simple and efficient method for purification of infectious recombinant adenovirus. *Jpn J. Med. Sci. Biol.* **47**, 157–166 (1994).
27. Nakano, M. *et al.* Efficient gene activation in cultured mammalian cells mediated by FLP recombinase-expressing recombinant adenovirus. *Nucleic Acids Res.* **29**, E40 (2001).
28. Fukuda, H., Terashima, M., Koshikawa, M., Kanegae, Y. & Saito, I. Possible mechanism of adenovirus generation from a cloned viral genome tagged with nucleotides at its ends. *Microbiol. Immunol.* **50**, 643–654 (2006).
29. Kim, D. W., Uetsuki, T., Kaziro, Y., Yamaguchi, N. & Sugano, S. Use of the human elongation factor 1 alpha promoter as a versatile and efficient expression system. *Gene* **91**, 217–223 (1990).
30. Chiyo, T. *et al.* Conditional gene expression in hepatitis C virus transgenic mice without induction of severe liver injury using a non-inflammatory Cre-expressing adenovirus. *Virus Res.* **160**, 89–97 (2011).
31. Kanegae, Y. *et al.* Efficient gene activation in mammalian cells by using recombinant adenovirus expressing site-specific Cre recombinase. *Nucleic Acids Res.* **23**, 3816–3821 (1995).
32. Takebe, Y. *et al.* SR alpha promoter: an efficient and versatile mammalian cDNA expression system composed of the simian virus 40 early promoter and the R-U5 segment of human T-cell leukemia virus type 1 long terminal repeat. *Mol. Cell Biol.* **8**, 466–472 (1988).
33. Saito, I., Groves, R., Giulotto, E., Rolfe, M. & Stark, G. R. Evolution and stability of chromosomal DNA coamplified with the CAD gene. *Mol. Cell Biol.* **9**, 2445–2452 (1989).

34. Nakano, M. *et al.* Production of viral vectors using recombinase-mediated cassette exchange. *Nucleic Acids Res.* **33**, e76 (2005).

Acknowledgements

We thank Ms M. Terashima for excellent technical support and Ms E. Kondo for secretarial assistance. This work was supported in part by Grants-in-Aid from the Ministry of Education, Culture, Sports, Science and Technology to Y.K. and S.K. and the Ministry of Health, Labour and welfare ; by Research on the innovative development and the practical application of new drugs for hepatitis B to I.S.

Author contributions

A.M. performed the experiments and contributed to the writing of the manuscript. Z.P., M.S., H.F., Y.O. and S.K. performed the experiments. I.S. discussed the data and wrote the manuscript. Y.K. designed the strategies and performed the experiments. All the authors discussed the results and commented on the manuscript.

Additional information

Supplementary information accompanies this paper at http://www.nature.com/scientificreports

Competing financial interests: The authors declare no competing financial interests.

How to cite this article: Maekawa, A. *et al.* Efficient production of adenovirus vector lacking genes of virus-associated RNAs that disturb cellular RNAi machinery. *Sci. Rep.* 3, 1136; DOI:10.1038/srep01136 (2013).

Virology 432 (2012) 29–38

Contents lists available at SciVerse ScienceDirect

Virology

journal homepage: www.elsevier.com/locate/yviro

Trans-complemented hepatitis C virus particles as a versatile tool for study of virus assembly and infection

Ryosuke Suzuki [a,*], Kenji Saito [a], Takanobu Kato [a], Masayuki Shirakura [b], Daisuke Akazawa [a], Koji Ishii [a], Hideki Aizaki [a], Yumi Kanegae [c], Yoshiharu Matsuura [d], Izumu Saito [c], Takaji Wakita [a], Tetsuro Suzuki [e,**]

[a] *Department of Virology II, National Institute of Infectious Diseases, 1-23-1 Toyama, Shinjuku-ku, Tokyo 162-8640, Japan*
[b] *Influenza Virus Research Center, National Institute of Infectious Diseases, Tokyo 208-0011, Japan*
[c] *Institute of Medical Science, University of Tokyo, Tokyo 108-8639, Japan*
[d] *Research Institute for Microbial Diseases, Osaka University, Osaka 565-0871, Japan*
[e] *Department of Infectious Diseases, Hamamatsu University School of Medicine, 1-20-1 Handayama, Higashi-ku, Hamamatsu, Shizuoka 431-3192, Japan*

ARTICLE INFO

Article history:
Received 30 March 2012
Returned to author for revisions
23 April 2012
Accepted 25 May 2012
Available online 22 June 2012

Keywords:
HCV
HCVtcp
Trans-packaging
Single-round infection

ABSTRACT

In this study, we compared the entry processes of *trans*-complemented hepatitis C virus particles (HCVtcp), cell culture-produced HCV (HCVcc) and HCV pseudoparticles (HCVpp). Anti-CD81 antibody reduced the entry of HCVtcp and HCVcc to almost background levels, and that of HCVpp by approximately 50%. Apolipoprotein E-dependent infection was observed with HCVtcp and HCVcc, but not with HCVpp, suggesting that the HCVtcp system is more relevant as a model of HCV infection than HCVpp. We improved the productivity of HCVtcp by introducing adapted mutations and by deleting sequences not required for replication from the subgenomic replicon construct. Furthermore, blind passage of the HCVtcp in packaging cells resulted in a novel mutation in the NS3 region, N1586D, which contributed to assembly of infectious virus. These results demonstrate that our plasmid-based system for efficient production of HCVtcp is beneficial for studying HCV life cycles, particularly in viral assembly and infection.

Introduction

Over 170 million people worldwide are chronically infected with hepatitis C virus (HCV), and are at risk of developing chronic liver diseases (Hoofnagle, 2002). HCV is an enveloped virus of the family *Flaviviridae*, and its genome is a positive-strand RNA consisting of the 5′-untranslated region (UTR), an open reading frame encoding viral proteins (core, E1, E2, p7, NS2, NS3, NS4A, NS4B, NS5A, and NS5B) and the 3′-UTR (Suzuki et al., 2007).

Host–virus interactions are required during the initial steps of viral infection. It was previously reported that CD81 (Bartosch et al., 2003a, b; McKeating et al., 2004; Pileri et al., 1998), scavenger receptor class B type I (Bartosch et al., 2003a, b; Scarselli et al., 2002), claudin-1 (Evans et al., 2007; Liu et al., 2009) and occludin (Benedicto et al., 2009; Evans et al., 2007; Liu et al., 2009; Ploss et al., 2009) are critical molecules for HCV entry into cells. CD81 interacts with HCV E2 via a second extracellular loop (Bartosch et al., 2003a, b; Hsu et al., 2003) and its role in the internalization process was confirmed (Cormier et al., 2004; Flint et al., 2006). It has also been shown that infectious HCV particles produced in cell cultures (HCVcc) exist as apolipoprotein E (ApoE)-enriched lipoprotein particles (Chang et al., 2007) and that ApoE is important for HCV infectivity (Owen et al., 2009).

Investigation of HCV had been hampered by difficulties in amplifying the virus in vitro before development of robust cell culture systems based on JFH-1 isolates (Lindenbach et al., 2005; Wakita et al., 2005; Zhong et al., 2005). Retrovirus-based HCV pseudoparticles (HCVpp), in which cell entry is dependent on HCV glycoproteins, have been used to study virus entry (Bartosch et al., 2003a; Hsu et al., 2003). Vesicular stomatitis virus (VSV)-based pseudotypic viruses bearing HCV E1 and E2 and replication-competent recombinant VSV encoding HCV envelopes have also been available as surrogate models for studies of HCV infection (Mazumdar et al., 2011; Tani et al., 2007).

It was recently shown that HCV subgenomic replicons can be packaged when structural proteins are supplied in *trans* (Adair et al., 2009; Ishii et al., 2008; Masaki et al., 2010; Steinmann et al., 2008). These *trans*-complemented HCV particles (HCVtcp) are infectious, but support only single-round infection and are unable to spread. Establishment of flexible systems to efficiently produce HCVtcp should contribute to studying HCV assembly, in particular encapsidation of the viral genome, and entry to cells with less stringent biosafety and biosecurity measures. Although single-round infection can be achieved by using the HCVcc system with receptor knock-out

* Corresponding author. Fax: +81 3 5285 1161.
** Corresponding author. Fax: +81 53 435 2338.
E-mail addresses: ryosuke@nih.go.jp (R. Suzuki), tesuzuki@hama-med.ac.jp (T. Suzuki).

0042-6822/$ - see front matter © 2012 Elsevier Inc. All rights reserved.
http://dx.doi.org/10.1016/j.virol.2012.05.033

cells, the single-round HCVcc system is not suitable for studying virus entry. We previously described plasmid-based production of HCVcc and HCVtcp (Masaki et al., 2010). Here, we demonstrated that HCVtcp production can be enhanced by introducing the previously reported cell-culture adaptive mutations and by deleting sequences not essential for replication in the subgenomic replicon construct. By providing genotype 1b-derived core-to-p7 in addition to intragenotypic viral proteins, chimeric HCVtcp were generated. Furthermore, blind passage of HCVtcp in the packaging cells resulted in the identification of a novel cell culture-adaptive mutation in NS3 that enables us to establish the efficient production of HCVtcp with structural proteins from various strains. Taken together, our system for producing single-cycle infectious HCV particles should be useful in the study of entry and assembly steps of the HCV life cycles. This technology may also have potential to be the basis for the safer vaccine development.

Results

Enhancement of HCVtcp production by adaptive mutations in E2, p7 and NS2 and by deleting sequences not essential for replication from replicon construct

In our HCVtcp system, the RNA polymerase I (Pol I)-driven replicon plasmid, which carries a dicistronic subgenomic luciferase reporter replicon of JFH-1 strain with a Pol I promoter and terminator (pHH/SGR-Luc), as well as a plasmid containing core-NS2 cDNA under the CAG promoter (pCAGC-NS2) were used (Masaki et al., 2010). In an effort to improve the yield of HCVtcp production, cell culture-adaptive mutations in E2 (N417S), p7 (N765D) and NS2 (Q1012R) which were previously selected from serial passage of HCVcc (Russell et al., 2008) were introduced into the core-NS2 expression plasmid (Fig. 1A) (residues are numbered

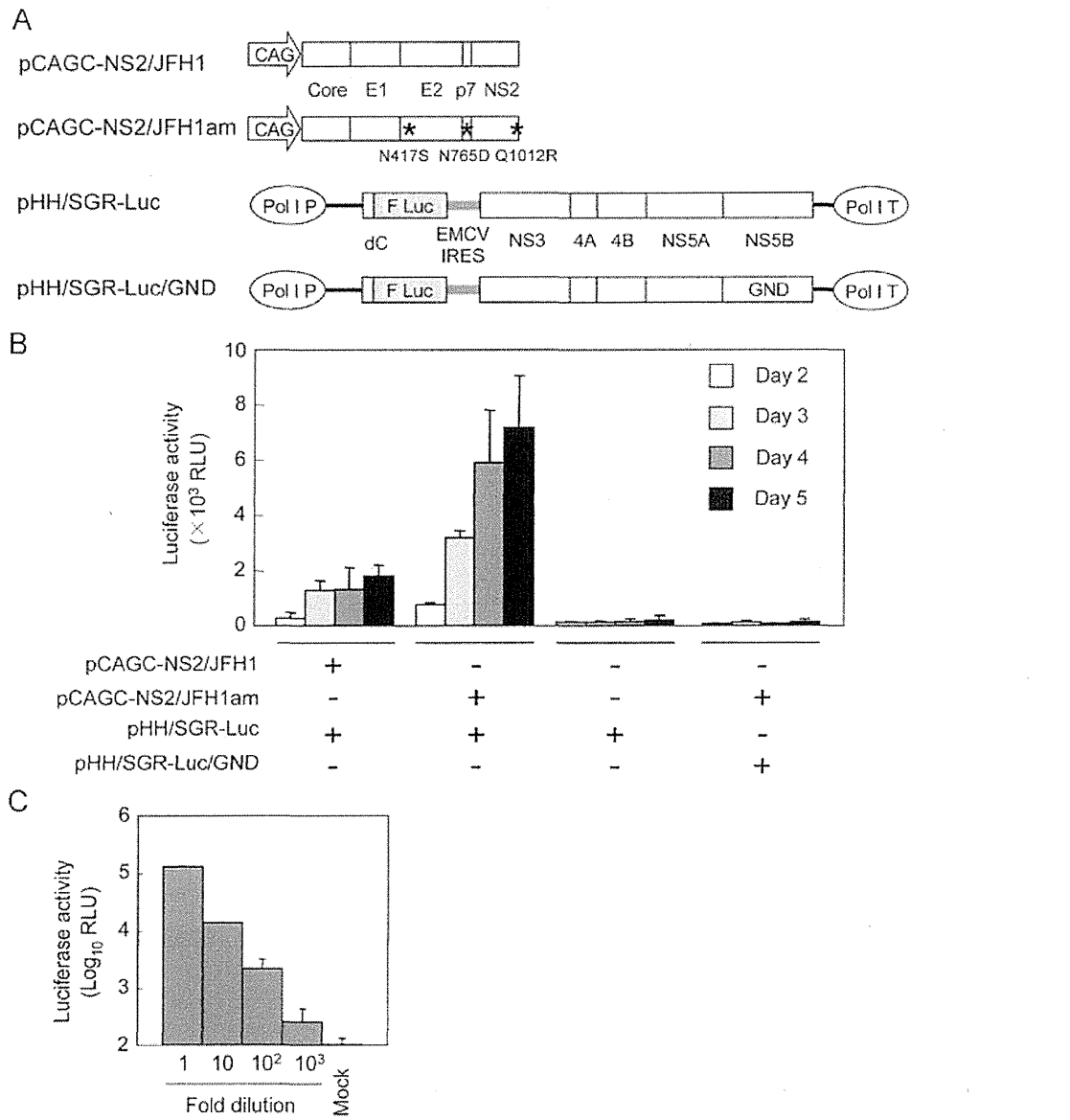

Fig. 1. HCVtcp production by two-plasmid transfection. (A) Schematic representation of plasmids is shown. HCV polyproteins derived from JFH-1 are indicated by white boxes. HCV UTRs are indicated by bold lines. The internal ribosomal entry site from encephalomyocarditis virus (EMCV IRES) is denoted as gray lines. Adaptive mutations are indicated as asterisks. F Luc: firefly luciferase gene; CAG: CAG promoter; Pol I P: RNA polymerase I promoter; Pol I T: RNA polymerase I terminator; GND: replication-deficient GND mutation. (B) Luciferase activity in Huh7.5.1 cells inoculated with supernatant from cells transfected with indicated plasmids at the indicated time points. Data are averages of triplicate values with error bars showing standard deviations. (C) Luciferase activity in cells inoculated with serially diluted HCVtcp.

according to positions within the JFH-1 polyprotein). Supernatants of cells transfected with plasmids (Fig. 1A) were collected and were used to infect Huh7.5.1 cells, which were analyzed by luciferase assay. Introduction of adaptive mutations (pCAGC-NS2/JFH1am) resulted in more than 4-fold higher production of HCVtcp at 5 day post-transfection, as compared to wild-type (WT) (pCAGC-NS2/JFH1) (Fig. 1B), indicating that the adaptive mutations contribute to enhancing HCVtcp production. To confirm that luciferase activity levels in HCVtcp-infected cells are correlated with the number of infectious particles, Huh7.5.1 cells were inoculated with serial dilutions of HCVtcp. Luciferase activity was well correlated with viral load (Fig. 1C), indicating that luciferase assay in HCVtcp-infected cells can be used to quantify HCV infection.

In order to further explore the efficient production of HCVtcp, we generated replicon constructs that lack the luciferase gene or include the partial coding sequences for structural proteins instead of reporter (Fig. 2A). Replication of each replicon in plasmid-transfected cells was then assessed by Western blotting (Fig. 2B). Among the constructs tested, NS5B levels were lowest in cells expressing pHH/SGR-Luc. NS5B levels in cells replicating other replicons appeared to be comparable. Cells were infected with supernatants of cells transfected with each replicon plasmid, along with pCAGC-NS2/JFH1am, followed by infectious unit assay (Fig. 2C). The highest production of HCVtcp was obtained from cells transfected with pHH/SGR, where the luciferase sequence was deleted from pHH/SGR-Luc, thus suggesting that deletion of the sequence not essential for RNA replication in the replicon may contribute to enhancing HCVtcp production.

Production of chimeric HCVtcp by providing heterologous core-p7

In order to elucidate whether *trans*-encapsidation of JFH-1 replicon can be achieved by providing core-p7 from other HCV strains, core-NS2 plasmids were constructed (Fig. 3A). In these plasmids, core through the N-terminal 33 aa of NS2, which contains transmembrane domain 1 of NS2, was derived from either H77c (genotype 1a), THpa (genotype 1b), Con1 (genotype 1b) or J6 (genotype 2a) strain. Residual NS2 was derived from JFH-1, as described previously (Pietschmann et al., 2006). HCVtcp was efficiently produced by core-p7 of J6 and THpa strains, but its production was less efficient in the case of Con1 strain. *Trans*-packaging was not detectable when core-p7 of H77c strain was used (Fig. 3C). Among HCV strains tested, difference in luciferase activity levels in HCVtcp-infected cells (Fig. 3C) were in agreement with that in the viral RNA levels in the culture supernatants of the transfected cells (Fig. 3B). Although the efficacy of *trans*-complementation was variable among strains, chimeric HCVtcp can be generated by providing genotype 1b-derived core-p7 in addition to intragenotypic viral proteins, and was used in subsequent studies.

ApoE- and CD81-dependent infection by HCVtcp

There is accumulating evidence that apolipoproteins, particularly ApoE, contribute to HCV production and infectivity (Chang et al., 2007; Owen et al., 2009). To determine whether ApoE is involved in infection of target cells by HCVtcp, we infected cells in the presence of increasing concentrations of anti-ApoE antibody.

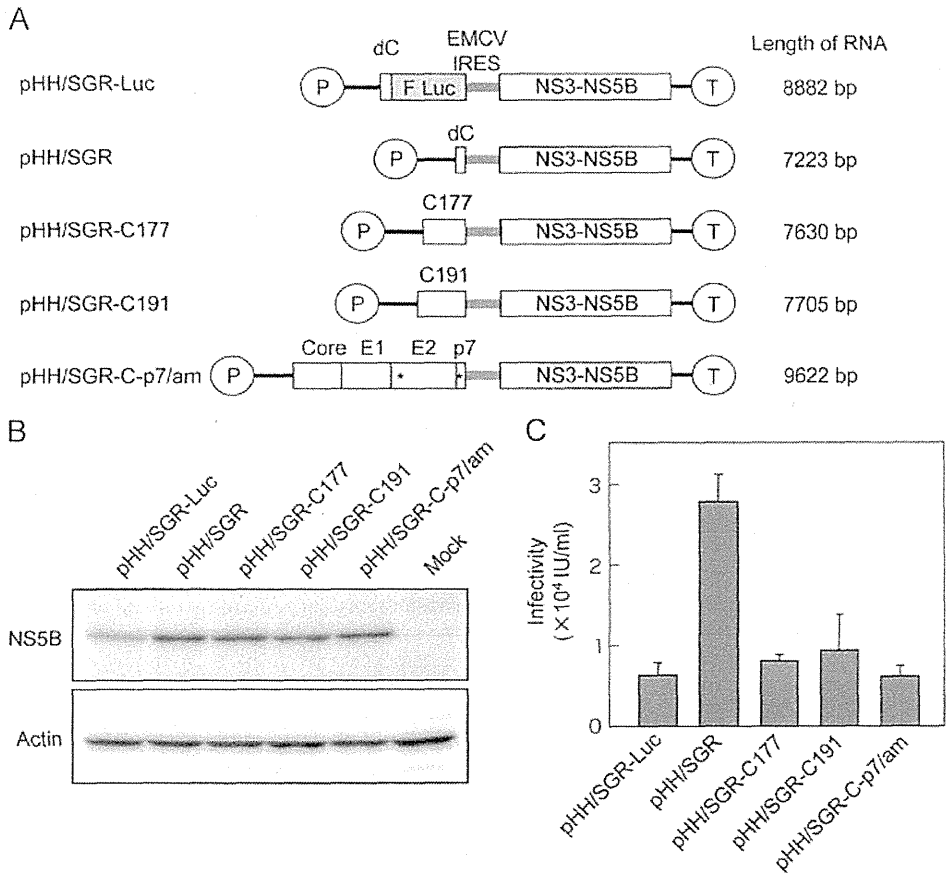

Fig. 2. Production of HCVtcp with different replicon constructs. (A) Schematic representation of plasmids used for production of HCVtcp. Deduced length of transcribed RNA from each construct is shown on the right. HCV polyproteins from JFH-1 strain are indicated by open boxes. HCV UTRs are indicated by bold lines. The EMCV IRES is denoted by gray bars. Adaptive mutations are indicated by asterisks. F Luc: firefly luciferase gene; P: RNA polymerase I promoter; T: RNA polymerase I terminator. (B) Detection of NS5B and actin in Huh7.5.1 cells transfected with indicated plasmids at 4 day post-transfection. (C) Infectivity of culture supernatants from cells transfected with indicated replicon plasmids along with pCAGC-NS2/JFH1am at 4 day post-transfection.

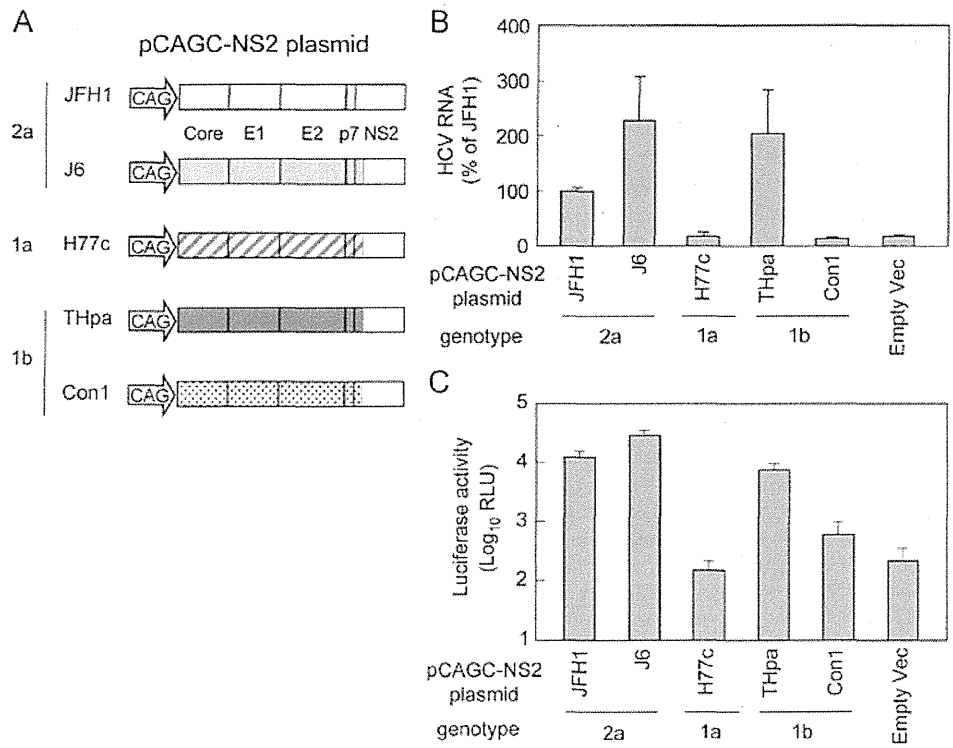

Fig. 3. HCVtcp production with structural proteins from various strains. (A) Schematic representation of plasmids used. HCV polyproteins of JFH-1, J6, H77c, THpa and Con1 strain are shown in the open box, bright gray box, box with diagonal lines, dark gray box and dotted box, respectively. (B) Relative levels of HCV RNA in the supernatant from cells transfected with indicated plasmids along with pHH/SGR-Luc. (C) Luciferase activity in cells inoculated with supernatant from cells transfected with indicated plasmids along with pHH/SGR-Luc at 4 day post-transfection.

pCAGC-NS2/THpa and pCAGC-NS2/JFH1am were used as core-NS2 plasmids for HCVtcp production carrying core-p7 derived from genotypes 1b and 2a (HCVtcp-1b and HCVtcp-2a, respectively). HCVpp derived from JFH-1 and VSVpp were generated and used for comparison. Infection with HCVtcp-1b or HCVtcp-2a was blocked by anti-ApoE antibody in a dose-dependent manner. In contrast, anti-ApoE antibody did not affect infection with HCVpp and VSVpp (Fig. 4A).

The CD81 dependence of infection was also compared between HCVtcp and HCVpp (Fig. 4B). Anti-CD81 antibody inhibited the entry of HCVtcp-1b, HCVtcp-2a, and HCVpp in a dose-dependent manner. The antibody had no effect on VSVpp infection. HCVtcp infection appears to be more sensitive to anti-CD81 antibody when compared with HCVpp infection; more than 60% inhibition was observed at 0.08 μg/mL anti-CD81 antibody for HCVtcp-1b and HCVtcp-2a, whereas approximately 50% inhibition was observed for HCVpp at 2 μg/mL antibody. Neutralization of HCVcc by anti-ApoE and anti-CD81 antibodies was also determined. Antibodies blocked HCVcc infection (Fig. 4C and D), as observed with HCVtcp. These results suggest that ApoE, as well as CD81, play an important role in HCVtcp infection. Thus, HCVtcp may be more useful for evaluating the HCV entry process than HCVpp.

Identification of novel culture-adaptive mutation in NS3 by serial passage of HCVtcp in packaging cells

The HCVtcp system was further applied to analyses of genetic changes during serial passages in target cells. As an initial attempt, supernatants of cells co-transfected with pCAGC-NS2/JFH1am and pHH/SGR were inoculated into Huh7.5.1 cells transiently transfected with pCAGC-NS2/JFH1am. However, infectious titer was lost after repeated inoculation, likely due to low HCVtcp titers and low efficiency of plasmid transduction (data not shown). To overcome this, we utilized recombinant adenovirus vectors (rAdVs) to provide core-NS2. As we were not able to obtain rAdV directly expressing core-NS2, conditional transgene expression based on a Cre-loxP strategy was employed (Kanegae et al., 1995). We constructed an rAdV containing core-NS2 gene downstream of a stuffer DNA flanked by a pair of loxP sites (AxCALNLH-CNS2). When cells were doubly infected with AxCALNLH-CNS2 and the Cre-expressing rAdV, AxCANCre (Kanegae et al., 1995), the Cre-mediated excisional deletion removed the stuffer DNA, resulting in core-NS2 expression under control of the CAG promoter (Fig. 5A). As expected, tightly regulated production of HCVtcp was observed. The cells infected with AxCANCre and AxCALNLH-CNS2 along with transduction of pHH/SGR-Luc produced HCVtcp at high levels. Production of HCVtcp was undetectable when either AxCANCre or AxCALNLH-CNS2 was not infected (Fig. 5B). The Cre-mediated rAdV expression system appears to have yielded considerably higher production of HCVtcp when compared with the settings for plasmid co-transfection.

Supernatants from cells in which core-NS2 was expressed using rAdVs and the subgenomic RNA derived from pHH/SGR replicated were inoculated into cells infected with AxCALNLH-CNS2 and AxCANCre (Fig. 6A). Blind passage was performed by sequentially transferring culture supernatants to cells infected with the above rAdVs. The two independent 10 blind passages (p10) showed virus titers of $> 1 \times 10^6$ IU/mL, which were markedly higher than those of the passage 0 (p0) stock cultures (4×10^4 IU/mL). Side-by-side infection analysis revealed that the HCVtcp p10 #1 achieved a virus titer approximately 36 times higher than that of HCVtcp p0 on the packaging cells at 6 day post-infection (Fig. 6B). Sequencing of the entire replicon in the supernatants at p10 in two independent experiments revealed

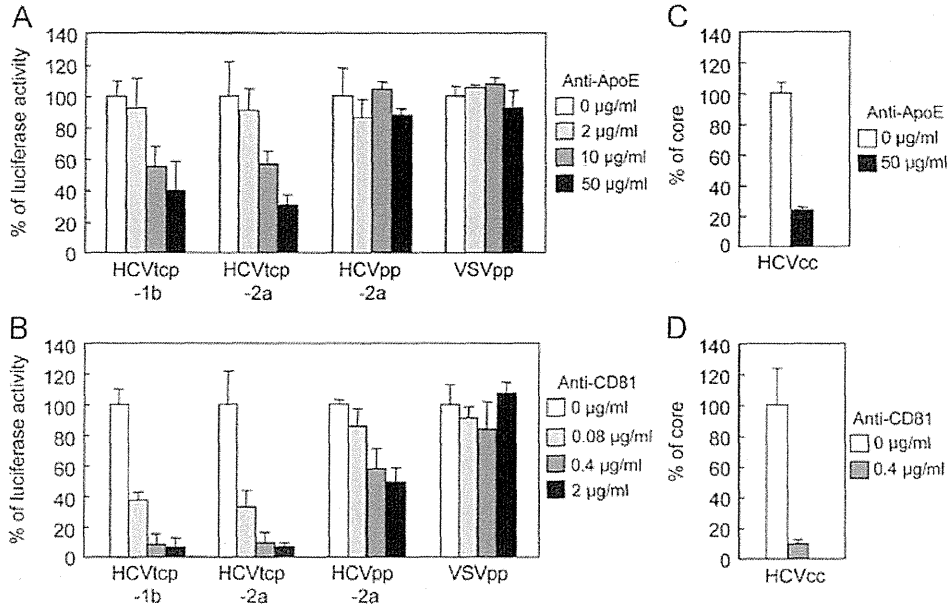

Fig. 4. Effects of anti-ApoE and anti-CD81 antibodies on HCV entry. (A) Aliquots of virus sample were incubated with increasing concentrations of anti-ApoE antibodies for 1 h and were then added to Huh7.5.1 cells. Luciferase activity was determined at 72 h post-infection and is expressed relative to activity without antibodies (white bar). (B) Huh7.5.1 cells were preincubated for 1 h with increasing concentrations of anti-CD81 antibodies, followed by inoculating virus samples. Luciferase activity was determined and expressed as shown in (A). (C) Aliquots of HCVcc were incubated with anti-ApoE antibodies for 1 h and were then added to Huh7.5.1 cells at an MOI of 0.05. Intracellular core levels were quantitated at 24 h post-infection and are expressed relative to levels without antibodies (white bar). (D) Huh7.5.1 cells were preincubated for 1 h with anti-CD81 antibodies. HCVcc infection and measurement of core proteins were performed as indicated in (C).

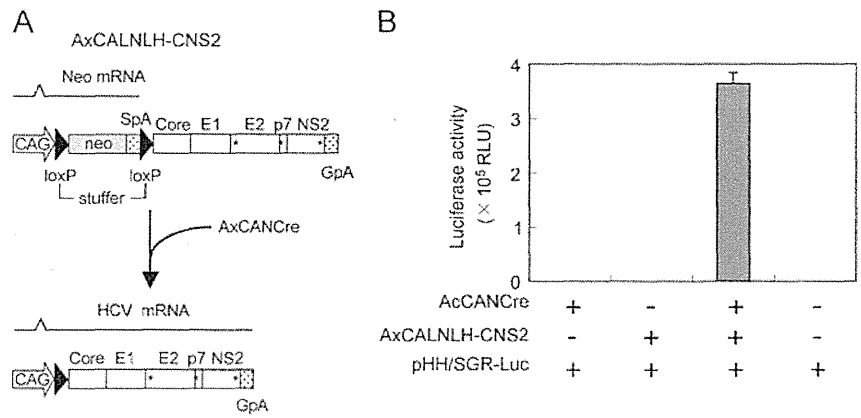

Fig. 5. Transgene activation mediated by rAdVs expressing Cre recombinase under control of CAG promoter. (A) Cre recobminase expressed by AxCANCre recognizes a pair of its target sequences loxP in AxCALNLH-CNS2, and removes the stuffer region resulting in expression of HCV core-NS2 polyprotein by CAG promoter. CAG: CAG promoter; SpA: SV40 early polyA signal; GpA: rabbit b-globin poly(A) signal. (B) Luciferase activity in Huh7.5.1 cells inoculated with 4-day post-transfection culture supernatant from cells transfected with pHH/SGR-Luc, and then infected with indicated rAdVs.

that both passaged HCVtcp had an identical nonsynonymous mutation in the NS3 region (N1586D) (Fig. 6C).

In order to examine the role of NS3 mutation identified on HCV RNA replication and on HCVtcp production, the N1586D mutation was introduced into pHH/SGR-Luc. Luciferase activities of the N1586D-mutated replicon were apparently lower than those of the WT-replicon, thus suggesting that the NS3 mutation reduced viral RNA replication (Fig. 7A). HCV RNA levels in the supernatants of cells transfected with WT- or mutant replicon plasmid along with pCAGC-NS2/JFH1am and luciferase activity in cells inoculated with supernatants from the transfected cells were then determined (Fig. 7B). The viral RNA level secreted from cells replicating the N1586D-mutated replicon was lower than that from cells replicating WT replicon (Fig. 7B, left). By contrast, a significantly higher infectivity of HCVtcp produced from the mutant replicon-cells was observed, as compared to WT replicon-cells (Fig. 7B, right), suggesting that the adaptive mutation increased the specific infectivity (almost 9-fold) of the virus particles. To further determine whether the N1586D mutation affects infectious viral assembly and/or virus release, we used the CD81-negative Huh-7 subclone, Huh7-25 (Akazawa et al., 2007), which may produce infectious particles, but is not susceptible to HCV entry due to a lack of CD81 expression, therefore allowing us to examine viral assembly and release without the influence of reinfection by produced HCVtcp. Measurement of intracellular and extracellular HCVtcp indicated that Huh7-25 cells replicating the N1586D-mutated replicon produced more infectious virus than WT in both supernatants and cell lysates (Fig. 7C). Thus, it can be concluded that the N1586D mutation contributes to enhanced infectious viral assembly, not RNA replication. We could not exclude the possibility that N1586D mutation affects virus release, since the mutation enhanced extracellular virus titers more than did the intracellular titer.

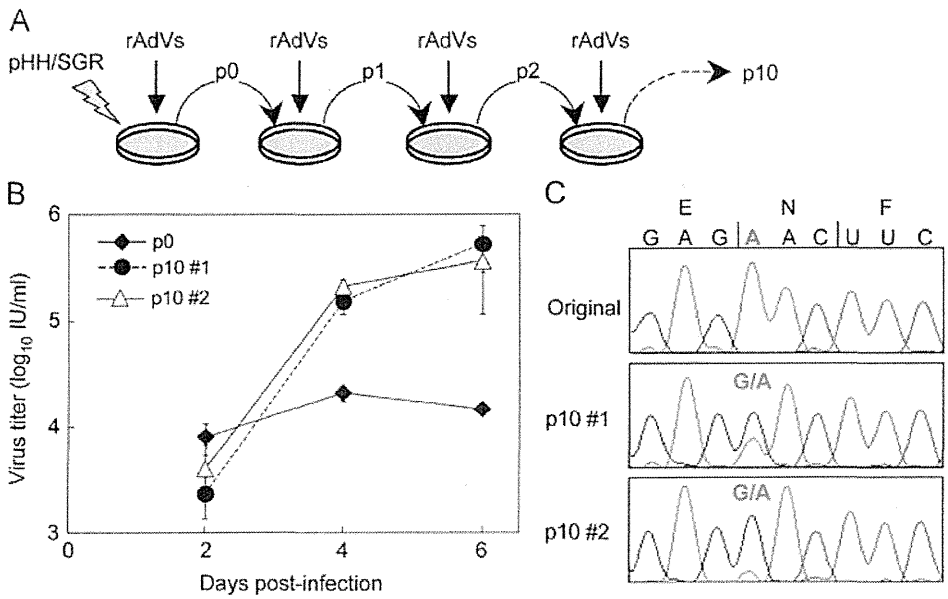

Fig. 6. Genotypic changes in HCVtcp following blind passage. (A) Experimental procedure for blind passage of HCVtcp. Huh7.5.1 cells were transfected with pHH/SGR and were doubly infected with AxCANCre and AxCALNLH-CNS2. Culture fluids were collected and were inoculated into cells infected with AxCANCre and AxCALNLH-CNS2. These procedures were repeated 10 times with two independent samples (#1 and #2). (B) Growth curves of HCVtcp p0 and p10 on Huh7.5.1 cells expressing core-NS2. Cells were infected with HCVtcp at an MOI of 0.05, and medium was collected at the indicated time points and subjected to titration. (C) Nucleotide sequences of original and blind-passaged replicons from HCVtcp. Nucleotides of mutated position are shown in red and bold.

The impact of the N1586D mutation on production of intra- and intergenotypic HCVtcp chimeras was also investigated. The N1586D mutation in the replicon enhanced the production of chimeric HCVtcp by providing core-p7 from all strains examined, although not statistically significant in THpa, and Con1 strains (Fig. 7D). Finally, to determine whether the N1586D mutation was responsible for enhancing HCVcc production, this mutation was introduced into pHHJFH1, which carries the full-length wild-type JFH-1 cDNA (Masaki et al., 2010), yielding pHHJFH1N1586D. The virus titer obtained from cells transfected with the pHHJFH1N1586D was significantly higher than that of WT (Fig. 7E), thus demonstrating that the N1586D mutation enhances yields of HCVcc, in addition to HCVtcp.

Discussion

Single-round infectious viral particles generated by *trans*-packaging systems are considered to be valuable tools for studying virus life cycles, particularly the steps related to entry into target cells, assembly and release of infectious particles. However, limited HCV strains have been applied for the efficient production of HCVtcp to date. In this study, we improved the HCVtcp system in order to enhance the productivity of infectious particles. Production of chimeric HCVtcp by providing genotype 1b-derived core-p7, in addition to intragenotypic viral proteins, was also confirmed. Furthermore, we exploited the system to investigate genetic changes during serial passage of target cells and identified a novel cell culture-adaptive mutation in NS3, which also contributes to enhance the productivity of HCVtcp.

HCVpp (Bartosch et al., 2003a; Hsu et al., 2003) has proven to be a valuable surrogate system by which the study of viral and cellular determinants of the viral entry pathway is possible. Early steps of HCV infection, including the role of HCV glycoprotein heterodimers, receptor binding, internalization and pH-dependent endosomal fusion, have been at least in part mimicked by HCVpp (Lavie et al., 2007). However, as HCVpp is generated in non-hepatic cells such as the human embryo kidney cells 293T, it is likely that the cell-derived component(s) of HCVpp differ from those of HCVcc. Hepatocytes play a role in maintaining lipid homeostasis in the body by assembling and secreting lipoproteins, including VLDL. It is highly likely that HCV exploits lipid synthesis pathways, as there is a tight link between virion formation and VLDL synthesis. Down-regulation of ApoE considerably reduces HCV production (Benga et al., 2010; Chang et al., 2007; Hishiki et al., 2010; Jiang and Luo, 2009; Owen et al., 2009). Infectivity of HCVcc is also neutralized by anti-ApoE antibodies (Chang et al., 2007). These data suggest that ApoE is important for HCV infectivity. Furthermore, Niemann-Pick C1-like 1 (NPC1L1), involving cholesterol uptake receptor, was recently identified as a host factor for HCV entry (Sainz et al., 2012). Knockdown of NPC1L1 had no effect on the entry of HCVpp whereas HCVcc entry was impaired, possibly due to different cholesterol content of these particles. Here, we found that the anti-ApoE antibody neutralized infection by HCVtcp and HCVcc, but not by HCVpp (Fig. 4A and C), thus suggesting that biogenesis and/or secretion pathways of VLDL are involved in HCVtcp similarly to HCVcc, but not in HCVpp.

We also observed that infectivity of HCVtcp and HCVcc is more efficiently neutralized by the anti-CD81 antibody, as compared to that of HCVpp (Fig. 4B and D). It has recently been reported that E2 of HCVcc contained both high-mannose-type and complex-type glycans, whereas most of the glycans on HCVpp-associated E2 were complex-type, which is matured by Golgi enzymes (Vieyres et al., 2010). Mutational analysis of the N-linked glycosylation sites in E1/E2 demonstrated that several glycans on E2 may affect the sensitivity of HCVpp against antibody neutralization, as well as access of CD81 to its binding site on E2 (Helle et al., 2010). The differences in sensitivity between HCVtcp and HCVpp to neutralization by anti-CD81 antibody observed here may be due to differences in carbohydrate composition of HCV glycoproteins during expression and processing of E1/E2 in cells and morphogenesis of HCVtcp and HCVpp.

By analyzing the various replicons for *trans*-packaging, we observed the highest production of HCVtcp with replicons from pHH/SGR, which lacked sequences not essential for RNA

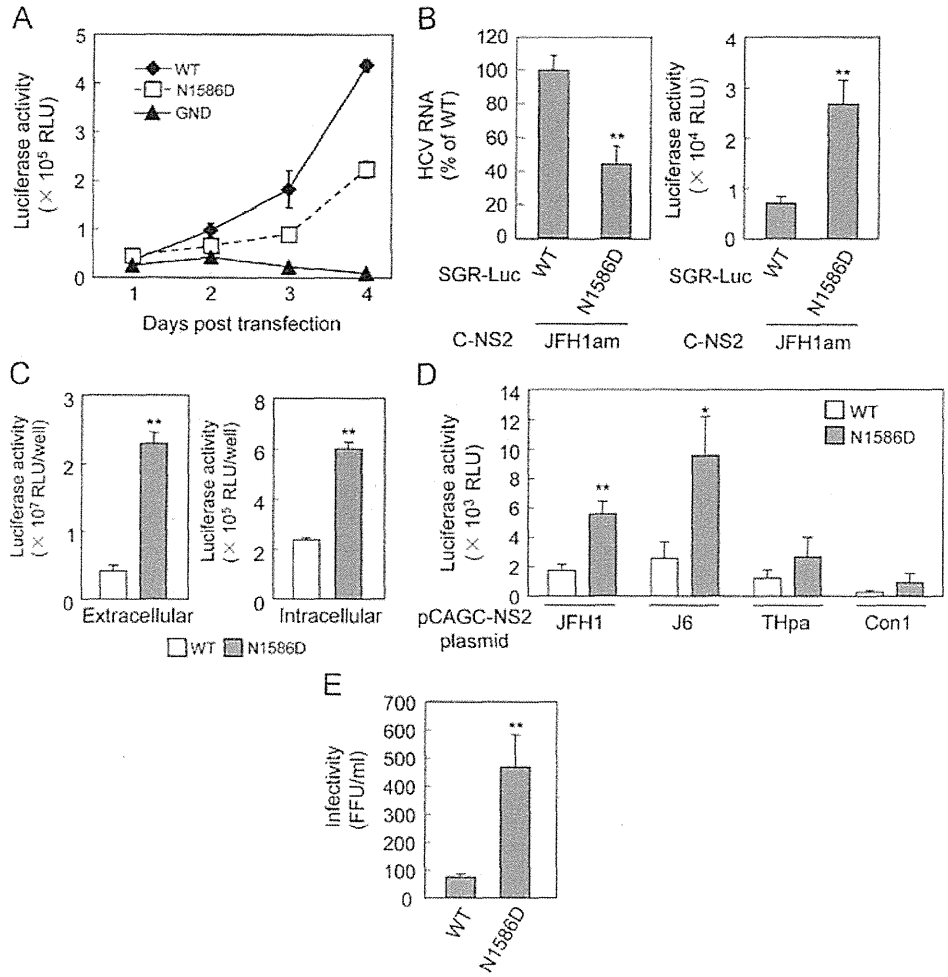

Fig. 7. Effects of N1586D mutation on RNA replication and production of HCVtcp or HCVcc. (A) RNA replication of replicons in cells transfected with pHH/SGR-Luc (WT) or N1586D mutant. Luciferase activities at 1 to 4 day post-transfection were determined. (B) Relative levels of HCV RNA in the supernatants from cells transfected with pHH/SGR-Luc (WT) or N1586D mutant plasmid along with pCAGC-NS2/JFH1am were shown in the left panel. Luciferase activities in cells inoculated with supernatants from cells transfected with indicated plasmids at 4 day post-transfection were shown in the right panel. (C) Luciferase activity in cells inoculated with supernatant and cell lysates from Huh7-25 cells transfected with pHH/SGR-Luc (WT) or N1586D mutant plasmid along with pCAGC-NS2/JFH1am at 5 day post-transfection. (D) Luciferase activity in cells inoculated with culture supernatant from cells transfected with pHH/SGR-Luc (WT) or N1586D mutant plasmid along with indicated core-NS2 plasmids at 4 day post-transfection. (E) Infectivity of supernatant from cells transfected with pHH/JFH1 (WT) or its derivative plasmid containing N1586D mutation at 6 day post-transfection. Statistical differences between WT and N1586D were evaluated using Student's *t*-test. $^{*}p < 0.05$, $^{**}p < 0.005$ vs. WT.

replication, while less efficient productivity was observed from pHH/SGR-Luc, pHH/SGR-C177, pHH/SGR-C191 and pHH/SGR-C-p7/am (Fig. 2C). Differences in the replication efficiency of the replicon do not appear to be a major determinant for HCVtcp productivity, at least in the present settings, as all replicon constructs except pHH/SGR-Luc replicated at similar levels, as confirmed by Western blotting (Fig. 2B). Although the shorter viral genome sequence may offer advantages over the longer sequence, further investigation is required in order to understand the molecular mechanisms underlying viral genome packaging. By comparing pHH/SGR vs. pHH/SGR-C177, pHH/SGR-C191 and pHH/SGR-C-p7/am, it is likely that the expression of the structural protein in *cis* does not increase HCVtcp production when sufficient amounts of structural proteins are supplied in *trans*.

Blind passage of HCVtcp in packaging cells infected with rAdVs providing core-NS2 enabled us to identify a novel culture-adaptive mutation in NS3. The N-terminal third of NS3 forms a serine protease, together with NS4A, and its C-terminal two-thirds exhibits RNA helicase and RNA-stimulated NTPase activities. In addition, similarly to flaviviruses (Kummerer and Rice, 2002; Liu et al., 2002), it is now apparent that HCV NS3 is also involved in viral morphogenesis (Han et al., 2009; Ma et al., 2008), although its precise role and underlying molecular mechanism(s) have not fully been elucidated. Two cell-culture adaptive NS3 mutations which are involved in HCV assembly have been identified. The Q1251L mutation in helicase subdomain 1 resulted in approximately 30-fold higher production of HCV without affecting NS3 enzymatic activities (Ma et al., 2008). The M1290K adaptive mutation was also located in subdomain 1 of the NS3 helicase (Han et al., 2009). The N1586D mutation identified here was located in subdomain 3 of helicase. Analogous to Q1251L and M1290K, the N1586D mutation enhanced the infectious viral assembly by increasing specific infectivity without affecting the efficiency of viral RNA replication. Considering the possibility that NS3 plays a role in linking between the viral replicase and assembly sites (Jones et al., 2011), it is likely that NS3 helicase is one of the determinants for interaction with the structural proteins. Our results, together with earlier studies, suggest that chimeric and defective mutations as well as supplying the viral components in *trans*, function as selective pressures in virion assembly.

In summary, we have established a plasmid-based reverse genetics for efficient production of HCVtcp with structural

proteins from various strains. Single-round infectious HCVtcp can complement the HCVcc and HCVpp systems as a valuable tool for the study of HCV life cycles.

Materials and methods

Cells

Huh7 derivative cell line Huh7.5.1 and Huh7-25 were maintained in Dulbecco modified Eagle medium (DMEM) supplemented with nonessential amino acids, 100 U of penicillin/mL, 100 μg of streptomycin/mL, and 10% fetal bovine serum at 37 °C in a 5% CO_2 incubator.

Plasmids

Plasmids pHHJFH1, pHH/SGR-Luc, pHH/SGR-Luc/GND and pCAG/C-NS2 were as described previously (Masaki et al., 2010). In this study, plasmid pCAG/C-NS2 was designated as pCAGC-NS2/JFH. The plasmid pCAGC-NS2/JFHam having adaptive mutations in E2 (N417S), p7 (N765D), and NS2 (Q1012R) in pCAGC-NS2/JFH was constructed by oligonucleotide-directed mutagenesis. These mutations were also introduced in pHHJFH1, resulting in pHHJFH1am. To generate core-NS2 expression plasmids with different strains of HCV, the cDNA coding core to the first transmembrane region of NS2 (33 amino acids) in pCAGC-NS2/JFH was replaced with the corresponding sequence of the J6 (Lindenbach et al., 2005), H77c (Yanagi et al., 1997), THpa (Shirakura et al., personal communication) and Con1 (Koch and Bartenschlager, 1999) strains. The THpa sequence contained the P to A mutation at 328 aa at E1 in the original TH strain. To generate pHH/SGR, pHH/SGR-Luc was digested with MluI and PmeI, followed by Klenow enzyme treatment and self-ligation to delete the luciferase coding sequence. To generate pHH/SGR-C177, pHH/SGR-C191 and pHH/SGR-C-p7/am, cDNA coding the partial core and luciferase in pHH/SGR-Luc were replaced with coding sequences for mature core (177aa), full-length core (191aa) or core-p7 polyprotein containing adaptive mutations in E2 and p7, respectively. The selected NS3 mutation (N1586D) was introduced into pHH/SGR-Luc and pHHJFH1 by oligonucleotide-directed mutagenesis.

Generation of viruses

HCVcc and HCVtcp were generated as described previously (Masaki et al., 2010). For the production of HCVpp-2a, plasmid pcDNAdeltaC-E1-E2(JFH1)am having adaptive mutations in E2 (N417S) in pcDNAdeltaC-E1-E2(JFH1) (Akazawa et al., 2007) was constructed by oligonucleotide-directed mutagenesis. Murine leukemia virus pseudotypes with VSV G glycoprotein expressing luciferase reporter (VSVpp) were generated in accordance with previously described methods (Akazawa et al., 2007; Bartosch et al., 2003a).

Luciferase assay

Huh7.5.1 cells were seeded onto a 24-well plate at a density of 3×10^4 cells/well 24 h prior to inoculation with reporter viruses. Cells were incubated for 72 h, followed by lysis with 100 μL of lysis buffer. Luciferase activity of the cells was determined using a luciferase assay system (Promega, Madison, WI). All luciferase assays were performed in triplicate.

Quantification of HCV infectivity and HCV RNA

To determine the titers of HCVtcp and HCVcc, Huh7.5.1 cell monolayers prepared in multi-well plates were incubated with dilutions of samples and then replaced with media containing 10% FBS and 0.8% carboxymethyl cellulose. Following incubation for 72 h, monolayers were fixed and immunostained with rabbit polyclonal anti-NS5A antibody, followed by Alexa Fluor 488-conjugated anti-rabbit secondary antibody (Invitrogen), and stained foci or individual cells were counted and used to calculate a titer of focus-forming units (FFU)/mL for spreading infections or infectious units (IU)/mL for non-spreading infections. For intracellular infectivity, the cell pellet was resuspended in culture media, and cells were lysed by four freeze–thaw cycles. Cell debris was pelleted by centrifugation for 5 min at 4000 rpm. Supernatant was collected and used for titration. To determine the amount of HCV RNA in culture supernatants, RNA was extracted from 140 μL of culture medium by QIAamp Viral RNA Mini Kit (QIAGEN, Valencia, CA) and treated with DNase (TURBO DNase; Ambion, Austin, TX) at 37 °C for 1 h. Extracted RNA was further purified by using an RNeasy Mini Kit, which includes RNase-free DNase digestion (QIAGEN). Copy numbers of HCV RNA were determined by real-time quantitative reverse transcription-PCR as described previously (Wakita et al., 2005).

Antibodies

Mouse monoclonal antibodies against actin (AC-15) and CD81 (JS-81) were obtained from Sigma (St. Louis, MO) and BD Biosciences (Franklin Lakes, NJ), respectively. Goat polyclonal antibody to ApoE (LV1479433) was obtained from Millipore (Tokyo, Japan). Anti-NS5A and anti-NS5B antibodies were rabbit polyclonal antibody against synthetic peptides.

Neutralization assay

For neutralization experiments with anti-CD81 antibody, Huh7.5.1 cells were incubated with dilutions of anti-CD81 antibody for 1 h at 37 °C. Cells were then infected with viruses for 5 h at 37 °C. For neutralization experiments with anti-ApoE antibody, viruses were incubated with various concentrations of anti-ApoE antibody at room temperature for 1 h and cells were infected with viruses for 5 h at 37 °C. Following infection, supernatant was removed and cells were incubated with culture medium, and luciferase activity was determined at 3 day post-infection for HCVtcp and pseudotyped viruses. For neutralization experiments with HCVcc generated with pHHJFH1am, a multiplicity of infection (MOI) of 0.05 was used for inoculation, and intracellular core protein levels were monitored by ELISA (Ortho Clinical Diagnostics) at 24 h post-infection.

Immunoblotting

Transfected cells were washed with PBS and incubated with lysis buffer (50 mM Tris–HCl, pH 7.4, 300 mM NaCl, 1% triton X-100). Lysates were then sonicated for 5 min and were added to the same volume of SDS sample buffer. Protein samples were boiled for 10 min, separated by SDS-PAGE, and transferred to PVDF membrane. After blocking, membranes were probed with first antibodies, followed by incubation with peroxidase-conjugated secondary antibody. Antigen–antibody complexes were visualized using an enhanced chemiluminescence detection system (Super Signal West Pico Chemiluminescent Substrate; PIERCE, Rockford, IL), in accordance with the manufacturer's protocols.

Generation of recombinant adenoviruses

rAdV, AxCANCre, expressing Cre recombinase tagged with nuclear localization signal under CAG promoter was prepared as described previously (Baba et al., 2005). The target rAdV AxCALNLH-CNS2 expressing HCV core-NS2 polyprotein with adaptive mutations in E2, p7 and NS2 was generated as follows. Cosmid pAxCALNLwit2 is identical to pAxCALNLw (Sato et al., 1998), except that both the terminal sequences of the rAdV genome are derived from pAxCAwit2 (Fukuda et al., 2006). The core-NS2 fragment obtained from pCAGC-NS2/JFH1am by StuI-EcoRI digestion and subsequent Klenow treatment was inserted into the SwaI site of pAxCALNLwit2. The resultant cosmid pAxCALNLH-CN2it2 was digested with PacI and transfected into 293 cells to generate rAdV AxCALNLH-CNS2.

Preparation of packaging cells for HCVtcp

Huh7.5.1 cells were coinfected with AxCANCre at an MOI of 1 and AxCALNLH-CNS2 at an MOI of 3 for expression of JFH-1 core-NS2 polyprotein containing the adaptive mutations in E2, p7 and NS2.

RNA preparation, RT-PCR and sequencing

Total cellular RNA was extracted with TRIzol reagent (Invitrogen, Carlsbad, CA), and subjected to reverse transcription with random hexamer and Superscript III reverse transcriptase (Invitrogen). Three fragments of HCV cDNAs that cover the entire HCV subgenomic replicon genome, were amplified by nested PCR with TaKaRa Ex Taq polymerase (Takara, Shiga, Japan). Amplified products were separated by agarose gel electrophoresis, and were used for direct DNA sequencing.

Acknowledgments

We are grateful to Francis V. Chisari (The Scripps Research Institute) for providing Huh7.5.1 cells. We thank M. Sasaki, M. Matsuda, and T. Date for their technical assistance, and T. Mizoguchi for the secretarial work. We also thank T. Masaki for their helpful discussions. This work was supported in part by grants-in-aid from the Ministry of Health, Labor, and Welfare and the Ministry of Education, Culture, Sports, Science, and Technology, Japan.

References

Adair, R., Patel, A.H., Corless, L., Griffin, S., Rowlands, D.J., McCormick, C.J., 2009. Expression of hepatitis C virus (HCV) structural proteins in trans facilitates encapsidation and transmission of HCV subgenomic RNA. J. Gen. Virol. 90 (Part 4), 833–842.

Akazawa, D., Date, T., Morikawa, K., Murayama, A., Miyamoto, M., Kaga, M., Barth, H., Baumert, T.F., Dubuisson, J., Wakita, T., 2007. CD81 expression is important for the permissiveness of Huh7 cell clones for heterogeneous hepatitis C virus infection. J. Virol. 81 (10), 5036–5045.

Baba, Y., Nakano, M., Yamada, Y., Saito, I., Kanegae, Y., 2005. Practical range of effective dose for Cre recombinase-expressing recombinant adenovirus without cell toxicity in mammalian cells. Microbiol. Immunol. 49 (6), 559–570.

Bartosch, B., Dubuisson, J., Cosset, F.L., 2003a. Infectious hepatitis C virus pseudoparticles containing functional E1-E2 envelope protein complexes. J. Exp. Med. 197 (5), 633–642.

Bartosch, B., Vitelli, A., Granier, C., Goujon, C., Dubuisson, J., Pascale, S., Scarselli, E., Cortese, R., Nicosia, A., Cosset, F.L., 2003b. Cell entry of hepatitis C virus requires a set of co-receptors that include the CD81 tetraspanin and the SR-B1 scavenger receptor. J. Biol. Chem. 278 (43), 41624–41630.

Benedicto, I., Molina-Jimenez, F., Bartosch, B., Cosset, F.L., Lavillette, D., Prieto, J., Moreno-Otero, R., Valenzuela-Fernandez, A., Aldabe, R., Lopez-Cabrera, M., Majano, P.L., 2009. The tight junction-associated protein occludin is required for a postbinding step in hepatitis C virus entry and infection. J. Virol. 83 (16), 8012–8020.

Benga, W.J., Krieger, S.E., Dimitrova, M., Zeisel, M.B., Parnot, M., Lupberger, J., Hildt, E., Luo, G., McLauchlan, J., Baumert, T.F., Schuster, C., 2010. Apolipoprotein E interacts with hepatitis C virus nonstructural protein 5A and determines assembly of infectious particles. Hepatology 51 (1), 43–53.

Chang, K.S., Jiang, J., Cai, Z., Luo, G., 2007. Human apolipoprotein E is required for infectivity and production of hepatitis C virus in cell culture. J. Virol. 81 (24), 13783–13793.

Cormier, E.G., Tsamis, F., Kajumo, F., Durso, R.J., Gardner, J.P., Dragic, T., 2004. CD81 is an entry coreceptor for hepatitis C virus. Proc. Natl. Acad. Sci. USA 101 (19), 7270–7274.

Evans, M.J., von Hahn, T., Tscherne, D.M., Syder, A.J., Panis, M., Wolk, B., Hatziioannou, T., McKeating, J.A., Bieniasz, P.D., Rice, C.M., 2007. Claudin-1 is a hepatitis C virus co-receptor required for a late step in entry. Nature 446 (7137), 801–805.

Flint, M., von Hahn, T., Zhang, J., Farquhar, M., Jones, C.T., Balfe, P., Rice, C.M., McKeating, J.A., 2006. Diverse CD81 proteins support hepatitis C virus infection. J. Virol. 80 (22), 11331–11342.

Fukuda, H., Terashima, M., Koshikawa, M., Kanegae, Y., Saito, I., 2006. Possible mechanism of adenovirus generation from a cloned viral genome tagged with nucleotides at its ends. Microbiol. Immunol. 50 (8), 643–654.

Han, Q., Xu, C., Wu, C., Zhu, W., Yang, R., Chen, X., 2009. Compensatory mutations in NS3 and NS5A proteins enhance the virus production capability of hepatitis C reporter virus. Virus Res. 145 (1), 63–73.

Helle, F., Vieyres, G., Elkrief, L., Popescu, C.I., Wychowski, C., Descamps, V., Castelain, S., Roingeard, P., Duverlie, G., Dubuisson, J., 2010. Role of N-linked glycans in the functions of hepatitis C virus envelope proteins incorporated into infectious virions. J. Virol. 84 (22), 11905–11915.

Hishiki, T., Shimizu, Y., Tobita, R., Sugiyama, K., Ogawa, K., Funami, K., Ohsaki, Y., Fujimoto, T., Takaku, H., Wakita, T., Baumert, T.F., Miyanari, Y., Shimotohno, K., 2010. Infectivity of hepatitis C virus is influenced by association with apolipoprotein E isoforms. J. Virol. 84 (22), 12048–12057.

Hoofnagle, J.H., 2002. Course and outcome of hepatitis C. Hepatology 36 (5 Suppl. 1), S21–9.

Hsu, M., Zhang, J., Flint, M., Logvinoff, C., Cheng-Mayer, C., Rice, C.M., McKeating, J.A., 2003. Hepatitis C virus glycoproteins mediate pH-dependent cell entry of pseudotyped retroviral particles. Proc. Natl. Acad. Sci. USA 100 (12), 7271–7276.

Ishii, K., Murakami, K., Hmwe, S.S., Zhang, B., Li, J., Shirakura, M., Morikawa, K., Suzuki, R., Miyamura, T., Wakita, T., Suzuki, T., 2008. Trans-encapsidation of hepatitis C virus subgenomic replicon RNA with viral structure proteins. Biochem. Biophys. Res. Commun. 371 (3), 446–450.

Jiang, J., Luo, G., 2009. Apolipoprotein E but not B is required for the formation of infectious hepatitis C virus particles. J. Virol. 83 (24), 12680–12691.

Jones, D.M., Atoom, A.M., Zhang, X., Kottilil, S., Russell, R.S., 2011. A genetic interaction between the core and NS3 proteins of hepatitis C virus is essential for production of infectious virus. J. Virol. 85 (23), 12351–12361.

Kanegae, Y., Lee, G., Sato, Y., Tanaka, M., Nakai, M., Sakaki, T., Sugano, S., Saito, I., 1995. Efficient gene activation in mammalian cells by using recombinant adenovirus expressing site-specific Cre recombinase. Nucl. Acids Res. 23 (19), 3816–3821.

Koch, J.O., Bartenschlager, R., 1999. Modulation of hepatitis C virus NS5A hyperphosphorylation by nonstructural proteins NS3, NS4A, and NS4B. J. Virol. 73 (9), 7138–7146.

Kummerer, B.M., Rice, C.M., 2002. Mutations in the yellow fever virus nonstructural protein NS2A selectively block production of infectious particles. J. Virol. 76 (10), 4773–4784.

Lavie, M., Goffard, A., Dubuisson, J., 2007. Assembly of a functional HCV glycoprotein heterodimer. Curr. Issues Mol. Biol. 9 (2), 71–86.

Lindenbach, B.D., Evans, M.J., Syder, A.J., Wolk, B., Tellinghuisen, T.L., Liu, C.C., Maruyama, T., Hynes, R.O., Burton, D.R., McKeating, J.A., Rice, C.M., 2005. Complete replication of hepatitis C virus in cell culture. Science 309 (5734), 623–626.

Liu, S., Yang, W., Shen, L., Turner, J.R., Coyne, C.B., Wang, T., 2009. Tight junction proteins claudin-1 and occludin control hepatitis C virus entry and are downregulated during infection to prevent superinfection. J. Virol. 83 (4), 2011–2014.

Liu, W.J., Sedlak, P.L., Kondratieva, N., Khromykh, A.A., 2002. Complementation analysis of the flavivirus Kunjin NS3 and NS5 proteins defines the minimal regions essential for formation of a replication complex and shows a requirement of NS3 in cis for virus assembly. J. Virol. 76 (21), 10766–10775.

Ma, Y., Yates, J., Liang, Y., Lemon, S.M., Yi, M., 2008. NS3 helicase domains involved in infectious intracellular hepatitis C virus particle assembly. J. Virol. 82 (15), 7624–7639.

Masaki, T., Suzuki, R., Saeed, M., Mori, K., Matsuda, M., Aizaki, H., Ishii, K., Maki, N., Miyamura, T., Matsuura, Y., Wakita, T., Suzuki, T., 2010. Production of infectious hepatitis C virus by using RNA polymerase I-mediated transcription. J. Virol. 84 (11), 5824–5835.

Mazumdar, B., Banerjee, A., Meyer, K., Ray, R., 2011. Hepatitis C virus E1 envelope glycoprotein interacts with apolipoproteins in facilitating entry into hepatocytes. Hepatology 54 (4), 1149–1156.

McKeating, J.A., Zhang, L.Q., Logvinoff, C., Flint, M., Zhang, J., Yu, J., Butera, D., Ho, D.D., Dustin, L.B., Rice, C.M., Balfe, P., 2004. Diverse hepatitis C virus glycoproteins mediate viral infection in a CD81-dependent manner. J. Virol. 78 (16), 8496–8505.

Owen, D.M., Huang, H., Ye, J., Gale Jr., M., 2009. Apolipoprotein E on hepatitis C virion facilitates infection through interaction with low-density lipoprotein receptor. Virology 394 (1), 99–108.

Pietschmann, T., Kaul, A., Koutsoudakis, G., Shavinskaya, A., Kallis, S., Steinmann, E., Abid, K., Negro, F., Dreux, M., Cosset, F.L., Bartenschlager, R., 2006. Construction and characterization of infectious intragenotypic and intergenotypic hepatitis C virus chimeras. Proc. Natl. Acad. Sci. USA 103 (19), 7408–7413.

Pileri, P., Uematsu, Y., Campagnoli, S., Galli, G., Falugi, F., Petracca, R., Weiner, A.J., Houghton, M., Rosa, D., Grandi, G., Abrignani, S., 1998. Binding of hepatitis C virus to CD81. Science 282 (5390), 938–941.

Ploss, A., Evans, M.J., Gaysinskaya, V.A., Panis, M., You, H., de Jong, Y.P., Rice, C.M., 2009. Human occludin is a hepatitis C virus entry factor required for infection of mouse cells. Nature 457 (7231), 882–886.

Russell, R.S., Meunier, J.C., Takikawa, S., Faulk, K., Engle, R.E., Bukh, J., Purcell, R.H., Emerson, S.U., 2008. Advantages of a single-cycle production assay to study cell culture-adaptive mutations of hepatitis C virus. Proc. Natl. Acad. Sci. USA 105 (11), 4370–4375.

Sainz Jr., B., Barretto, N., Martin, D.N., Hiraga, N., Imamura, M., Hussain, S., Marsh, K.A., Yu, X., Chayama, K., Alrefai, W.A., Uprichard, S.L., 2012. Identification of the Niemann-Pick C1-like 1 cholesterol absorption receptor as a new hepatitis C virus entry factor. Nat. Med. 18 (2), 281–285.

Sato, Y., Tanaka, K., Lee, G., Kanegae, Y., Sakai, Y., Kaneko, S., Nakabayashi, H., Tamaoki, T., Saito, I., 1998. Enhanced and specific gene expression via tissue-specific production of Cre recombinase using adenovirus vector. Biochem. Biophys. Res. Commun. 244 (2), 455–462.

Scarselli, E., Ansuini, H., Cerino, R., Roccasecca, R.M., Acali, S., Filocamo, G., Traboni, C., Nicosia, A., Cortese, R., Vitelli, A., 2002. The human scavenger receptor class B type I is a novel candidate receptor for the hepatitis C virus. EMBO J. 21 (19), 5017–5025.

Steinmann, E., Brohm, C., Kallis, S., Bartenschlager, R., Pietschmann, T., 2008. Efficient trans-encapsidation of hepatitis C virus RNAs into infectious virus-like particles. J. Virol. 82 (14), 7034–7046.

Suzuki, T., Ishii, K., Aizaki, H., Wakita, T., 2007. Hepatitis C viral life cycle. Adv. Drug Deliv. Rev. 59 (12), 1200–1212.

Tani, H., Komoda, Y., Matsuo, E., Suzuki, K., Hamamoto, I., Yamashita, T., Moriishi, K., Fujiyama, K., Kanto, T., Hayashi, N., Owsianka, A., Patel, A.H., Whitt, M.A., Matsuura, Y., 2007. Replication-competent recombinant vesicular stomatitis virus encoding hepatitis C virus envelope proteins. J. Virol. 81 (16), 8601–8612.

Vieyres, G., Thomas, X., Descamps, V., Duverlie, G., Patel, A.H., Dubuisson, J., 2010. Characterization of the envelope glycoproteins associated with infectious hepatitis C virus. J. Virol. 84 (19), 10159–10168.

Wakita, T., Pietschmann, T., Kato, T., Date, T., Miyamoto, M., Zhao, Z., Murthy, K., Habermann, A., Krausslich, H.G., Mizokami, M., Bartenschlager, R., Liang, T.J., 2005. Production of infectious hepatitis C virus in tissue culture from a cloned viral genome. Nat. Med. 11 (7), 791–796.

Yanagi, M., Purcell, R.H., Emerson, S.U., Bukh, J., 1997. Transcripts from a single full-length cDNA clone of hepatitis C virus are infectious when directly transfected into the liver of a chimpanzee. Proc. Natl. Acad. Sci. USA 94 (16), 8738–8743.

Zhong, J., Gastaminza, P., Cheng, G., Kapadia, S., Kato, T., Burton, D.R., Wieland, S.F., Uprichard, S.L., Wakita, T., Chisari, F.V., 2005. Robust hepatitis C virus infection in vitro. Proc. Natl. Acad. Sci. USA 102 (26), 9294–9299.

Biochemical and Biophysical Research Communications 417 (2012) 945–950

Contents lists available at SciVerse ScienceDirect

Biochemical and Biophysical Research Communications

journal homepage: www.elsevier.com/locate/ybbrc

Copy number of adenoviral vector genome transduced into target cells can be measured using quantitative PCR: Application to vector titration

Zheng Pei, Saki Kondo, Yumi Kanegae, Izumu Saito *

Laboratory of Molecular Genetics, Institute of Medical Science, University of Tokyo, 4-6-1 Shirokanedai, Minato-ku, Tokyo 108-8639, Japan

ARTICLE INFO

Article history:
Received 25 November 2011
Available online 19 December 2011

Keywords:
Adenovirus vector
Virus titer
Quantitative PCR

ABSTRACT

Both transfection and adenovirus vectors are commonly used in studies measuring gene expression. However, the real DNA copy number that is actually transduced into target cells cannot be measured using quantitative PCR because attached DNA present on the cell surface is difficult to distinguish from successfully transduced DNA. Here, we used Cre/*lox*P system to show that most of the transfected DNA was in fact attached to the cell surface; in contrast, most of the viral vector DNA used to infect the target cells was present inside the cells after the cells were washed according to the conventional infection protocol. We applied this characteristic to adenoviral vector titration. Current methods of vector titration using the growth of 293 cells are influenced by the effect of the expressed gene product as well as the cell conditions and culture techniques. The titration method proposed here indicates the copy numbers introduced to the target cells using a control vector that is infected in parallel (relative vector titer: rVT). Moreover, the new titration method is simple and reliable and may replace the current titration methods of viral vectors.

1. Introduction

Transfection is the most commonly used method of choice for examining the nature and function of a gene *in vivo* because this technique is very simple to perform and easy to manipulate. However, the copy numbers of DNA that successfully reach the inside of the target cells cannot be measured using quantitative PCR (qPCR), since experiments using qPCR cannot effectively distinguish DNA present inside the cells from DNA attached to and present on the cell surface. The first-generation adenovirus vector (FG AdV) is now commonly used for gene expression experiments, mainly because the resulting expression level is much higher than that achieved using transfection. Another reason is that the data offered by this vector is quantitative for a linearity range that is about 20-fold wider [1]. However, the vector system is also thought to be unsuitable for qPCR for the same reason mentioned above.

There are several methods for using FG AdV. The most popular titration methods are bioassays of plaque-forming unit (PFU) [2,3] and end-point cytopathic effect (CPE) assay or 50% tissue-culture infectious dose ($TCID_{50}$) assay [3,4]. These methods were actually developed for the titration of wild-type adenoviruses, and not for the titration of FG AdV. At least 4 days or up to 2 weeks are required to obtain the endpoint, and the results often vary depending on the conditions of the 293 cell lines, researchers and laboratories. The immunofluorescent focus assay using a florescent microscope [5,6] and the immunospot assay using 3,3′-diaminobenzidine staining [7] (TaKaRa Bio kit), count the foci of infected 293 cells expressing viral hexon protein. Although the titration can be completed in 2 days, these methods also rely on viral replication in 293 cells. The amount of AdV particles has been measured based on the optical density at 260 nm (OD_{260}) [8], although this method can only be used for purified virus stock. Because the AdVs replicate rapidly in growing 293 cells in all these methods, the titration results are sometimes influenced by the expressed product of an inserted gene if it disturbs viral replication or the growth of 293 cells. Consequently, sometimes the results do not reflect the actual copy number that was transferred to the target cells, which is undoubtedly the most important ability of a "vector".

qPCR has been used to calculate the copy numbers of AdV in viral stocks [9]. In the preparation of helper-dependent AdV (HD AdV), the contaminated helper virus (an FG AdV) in the viral stock has been measured using qPCR [10,11]. Another category of the qPCR method obtains the viral titer not by measuring AdV DNA in the viral stock, but by quantifying the copy numbers of *transduced viral genomes in the target cells* (genomic infectious titer,

Abbreviations: FG, first-generation; AdV, adenoviral vector; PFU, plaque-forming unit; $TCID_{50}$, 50% tissue-culture infectious dose; CPE, cytopathic effect; qPCR, quantitative real-time PCR; HD-AdV, helper-dependent AdV; GIT, genomic infectious titer; rVT, relative vector titer; MOI, multiplicity of infection; NLS, nuclear localization signal; OTC, Ornithine transcarbamylase.

* Corresponding author. Fax: +81 3 5449 5432.
E-mail address: isaito@ims.u-tokyo.ac.jp (I. Saito).

0006-291X/$ - see front matter © 2011 Elsevier Inc. All rights reserved.
doi:10.1016/j.bbrc.2011.12.016

GIT); the total DNA of the infected cells were extracted, and the viral DNA were detected using slot-blot hybridization [12] or qPCR [10,13]. Although all these methods are intended to measure the copy number of the viral genome, there are two problems with using them for the titration of FG AdV. One reason is similar to that described above for transfection but is more crucial: the obtained copy numbers include not only the viral genome of the internally transduced viral particles, but also the DNA of *non-infectious particles* and unpackaged naked DNA that is present either freely in the viral stock or attached to the surface of the target cells. The other problem is that the GIT fluctuates markedly depending on the target cell concentration and conditions; hence, GITs obtained at different times and places are difficult to compare. Therefore, both of these problems must be solved to establish a reliable GIT method. In this paper, we propose a new titration method that solves these problems.

2. Materials and methods

2.1. Cell lines and recombinant adenovirus

The human embryo kidney cell line 293 [14] constitutively expresses adenoviral E1 genes. The cell line CV-1 is derived from African green monkey kidney. HeLa cells are derived from human cervical cancer. The cell line NIH-3T3 was established from an NIH Swiss mouse embryo. AxCANCre, a Cre-expressing AdV tagged with a nuclear localization signal [15], and AxEFdsR, a dsRed-expressing AdV [16], have been described previously. The GFP-expressing AdV AxCAGFP was generated using the COS-TPC method [17]. The AdV AxEFLNLdsRed is identical to AxCALNLZ [15] except that the CAG promoter and the LacZ gene were replaced by the EF1α promoter, and the dsRed gene, respectively. The $TCID_{50}$ was measured according to the protocol described by Kanegae et al. [4]. The plasmid pA14cw contains the AdV genomic DNA of pAdex1w [17] from map units 0 to 14.

2.2. Southern blotting analysis

CV-1 cells in a 6-cm dish were infected with AxCANCre. After 24 h, the cells were infected with AxEFLNLdsRed or transfected with 1 μg of the plasmid pxEFLNLdsRed per 6-cm dish using Transfast (Promega). The total DNA was prepared from the dish [18]. Before alkaline treatment, the agarose gel was exposed to 0.1-N HCl for partial depurination causing DNA fragmentation to several hundred base pairs (bp) to obtain the complete transfer to the membrane [19]; the DNA was then transferred to the nylon membrane Hybond-N (Amersham GE) using the capillary-transfer method [20]. Specific DNA was detected using a DIGDNA Labeling and Detection Kit (Roche Diagnostics). The 0.6-kb *XmnI* fragment derived from the EF1α promoter region was labeled with digoxigenin-UTP, and specific DNA was detected using the chemiluminescence of CDP-Star (Roche Diagnostics). The bands were visualized using LAS-4000 (Fuji Film) and the densitometry was performed using an image analysis program (Multi Gauge version 3X, Fuji Film). The linear correlation between the DNA amounts and the intensity of the bands was confirmed (Fig. S1 of Supplementary Data), showing that the Southern analysis was quantitative.

2.3. qPCR

The infected total cell DNA was prepared from cells, as described previously [18,21]. Alternatively, we confirmed the total cell DNA prepared using a DNA preparation kit (Macherey–Nagel through TaKaRa Bio). qPCR was performed to detect the AdV genome using a probe for the pIX gene [16] (Fig. 2A). The amount of chromosomal DNA was simultaneously measured to correct the Ct values of the viral genome per cell, and the corrected Ct was shown throughout. The probes were derived from the sequence of the human β-actin gene for HeLa, the human OTC gene for CV-1 [16], and the mouse GAPDH gene for NIH-3T3 (Applied Biosystems, catalog number 7000-1). The qPCR reaction was performed according to the manufacturer's protocol: 50 °C for 2 min and 95 °C for 10 min, followed by 40 cycles of 95 °C for 15 s and 60 °C for 1 min (Applied BioSystems).

2.4. Generation of a standard curve using qPCR

The copy numbers of the plasmid pA14cw containing the pIX sequences and the cosmid pAxcwit2 [22] containing the full-genome of the FG AdV [22] were calculated according to Puntel et al. [11]. The plasmid and cosmid were serially diluted (Fig. 2B and C). The equivalency between the molecular weight of the plasmid pA14cw and the number of copies was calculated by considering the pA14cw molecular weight and the equivalency between base pairs (pA14cw [4,247 bp]) and Daltons (Da) ($1bp_{Ads} = 678$ Da). $Mass_{pA14cw}$ (Da) = 4,247 bp/molecule × 678 Da/bp = 2.88×10^6 Da/molecule. We obtained the equivalency of mass 2.88×10^6 Da/molecule × 1.66×10^{-18} μg/Da = 4.78×10^{-12} μg/molecule. The copy numbers of the cosmid pAxcwit2 (42, 698 bp) were similarly calculated.

3. Results and discussion

3.1. Quantification of internally transduced viral copies in target cells

To establish a reliable GIT method, determining the ratio of successfully internalized viral DNA to DNA that has physically attached to the cell surface (that is, naked viral DNA or DNA in inactivated viral particles in AdV-infected target cells) is essential. To estimate the amounts of the former and the latter, we utilized the Cre/*lox*P system. CV-1 cells were infected with the AdV AxCANCre expressing Cre at an MOI of 5. Then, 24 h later, the cells were infected with the target AdV AxEFLNLdsRed at an MOI of 7.5 or were transfected with 1 μg of the target plasmid pxEFLNLdsRed as a control. The target unit in the AdV and the plasmid contains the same sequences of the EF1α promoter and the dsRed gene flanked by two *lox*Ps (Fig. 1A). The total cell DNA was extracted after the indicated number of days and digested with *BglII*; the DNA of the target unit was detected using a Southern technique (Fig. 1B and C). The 2.8-kb band (S2.8) indicates the substrate originally present before Cre-mediated recombination, i.e., the unprocessed substrate, while the 1.5-kb band (R1.5) shows the presence of the recombined product. We considered that the viral DNA and the transfected DNA that are physically attached to the cell surface cannot be processed by Cre and remain as unprocessed substrate.

When the cells were transfected with the target plasmid, the majority of the target DNA remained unprocessed even after 72 h (Fig. 1C, column 6). A densitometry analysis showed that only 9 ± 2% ($n = 7$) of the DNA was processed substrate. Also, a preliminary experiment showed that when using 3 μg of plasmid DNA, the percentage was 12% (data not shown). These results suggested that most of the transfected DNA was possibly present on the cell surface and that the DNA copy number after transfection did not reflect that of the internalized DNA molecules. In contrast, most of the target viral DNA was processed using Cre-mediated recombination by 2 or 3 days after infection (Fig. 1B, columns 5 and 6); the recombination efficiency was 92 ± 3% ($n = 4$). Considering that the recombination efficiency must not be 100%, the result suggested that at least 92% of the target viral DNA was present inside the infected cells. Similar results were obtained when using

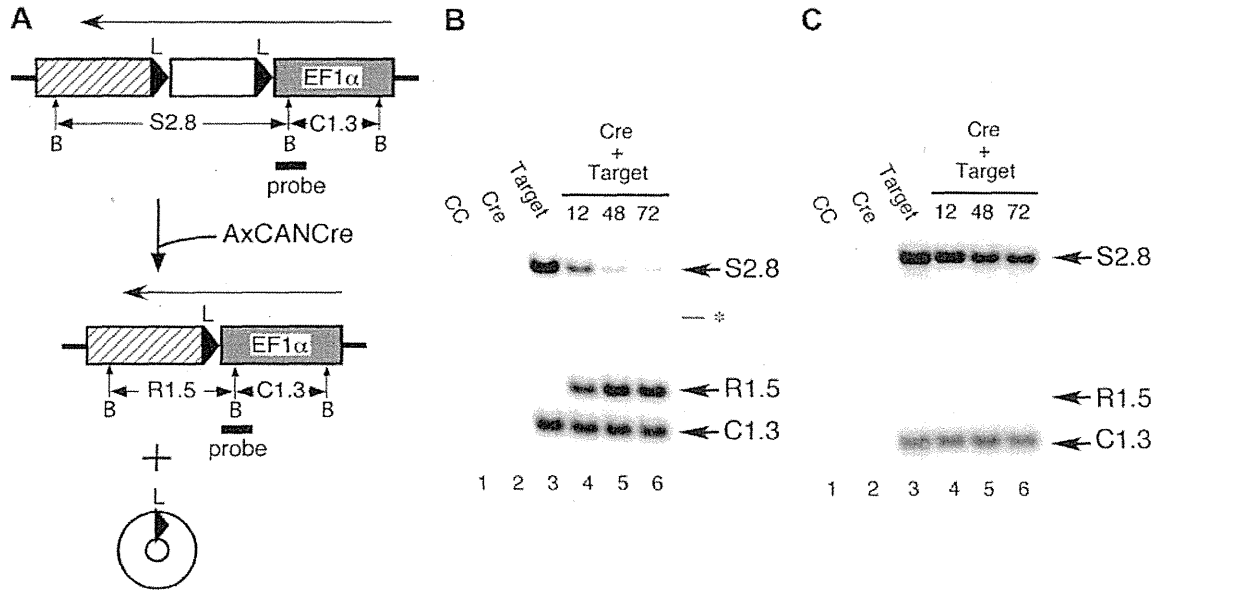

Fig. 1. (A) Structure of the target unit of recipient virus and plasmid. White box, stuffer DNA consisting of neo gene plus polyadenylation (poly(A)) sequence; shadowed box, cDNA plus poly(A) sequence; solid triangle, *lox*P sequence. Arrows show the direction of transcription. (B) Cre-mediated recombination using AdV. CC, uninfected; Cre, AxCANCre; Target, AxEFLNLdsRed. The numbers show the hours after infection. The asterisk shows the sequence of the EF1α gene in the human chromosome. (C) Cre-mediated recombination using plasmid transfection. The representations are the same in (B). For the densitometry four and seven independent experiments in (B) and (C) were performed, respectively.

different MOIs from 1 to 10 (Fig. S2). Therefore, the result showed that nearly all the detected viral DNA was derived from internalized, actively infectious viral particles; hence, the quantification of viral genomes using qPCR can be reliably used for titration.

3.2. Measurement of AdV-genome copies in infected cells using qPCR

A set of TaqMan PCR primers and probes were designed for detecting the AdV genome in the viral pIX coding region, since this gene is present closest to the target insert and encodes a viral structural protein that is essential for stable viral particles (Fig. 2A). The method for quantifying the copy number of FG AdV DNA in infected cells was essentially that described by Ma et al. [9]. The sensitivity of detection and the linear range of the quantification of this qPCR were determined by serial dilution of the 4.2-kb plasmid pA14cw containing the pIX gene and the 42.7-kb cosmid pAxcwit2 containing the full-length genome of the AdV backbone (Fig. 2B and C). The linear range for quantification was found to be between at least 10^3 and 10^9 copies for the plasmid template pA14cw per 5 μL; a plot of the plasmid copy number versus the Ct value between 7 and 27 was linear on a logarithmic scale with a coefficient correlation (r^2) of 0.99 (Fig. 2B). The cosmid template Axcwit2 produced an identical result (Fig. 2C), confirming that the Ct value accurately depended on the copy numbers irrespective of the DNA size. Based on these results, the Ct values obtained using our PCR system can be converted to the copy numbers for a given DNA sample.

As the next step in the titration using qPCR, CV-1 cells in the well of a 24-well plate (2.0×10^5 cells) were infected using the suspension method (see below) with 10 μL of serially diluted stocks of AxCAGFP virus ("control virus stock" for the conversion of the viral Ct value to the copy number *when using our particular qPCR machine*), and the total infected cell DNA was extracted and the Ct values of the viral genome corrected using the Ct value of the cell DNA (see Section 2) were measured (Fig. 2D). A linear correlation of the Ct values to the dilutions was observed from 18 to at least 28. Therefore, together with the results shown in Fig. 2C, the GIT, i.e., the copy number of the transduced viral genome per cell for this cell concentration of 2.0×10^5 cells, can be calculated. For example, a 10^{-2} dilution of 10 μL of viral stock produced a Ct value of 24.34 according to the equation shown in Fig. 2D ($y = 2.97x + 18.4$), and the same Ct value using that shown in Fig. 2C ($y = 24.34 = -3.4x + 38.2$) corresponded to $10^{4.08} \approx 1.2 \times 10^4$ copies of viral genome in 5 μL, i.e., *the GIT titer of the control virus stock was* 2.4×10^8 *copies/mL* ($1.2 \times 10^4 \times 10^3/5 \times 1/10^{-2}$). As described above, because the equations for the plasmid (Fig. 2B) and the cosmid (Fig. 2C) were practically identical, not the cosmid but a plasmid containing the pIX gene can be used for the conversion of the vital Ct value to the copy number. This method of obtaining the GIT of a control virus is essential for rVT because the Ct value differs depending on the qPCR machine. If the $TCID_{50}$ titer of this control virus is known, the $TCID_{50}$ titer can be converted to the copy number/mL (see Section 3.5).

3.3. Establishment of the method for relative vector titer (rVT)

To examine the effect of the cell concentration on the GIT, HeLa cells at densities of 0.6, 2.0 and 6.0×10^5 (full sheet condition) per 6-well plate were infected in parallel with a virus of unknown titer (testing virus) and the virus AxCAGFP (control virus, the same virus used in Fig. 2D). Three days later, the total cell DNA was extracted. For each DNA sample, the Ct values of not only the viral DNA but also the cell chromosome DNA were simultaneously measured to correct for fluctuations in the cell numbers (see Section 2). The transduced copy numbers/mL, i.e. the GIT, vary markedly from 1 to 3.2 and 4.9 in their ratio as reported by Sandig et al. [13] (columns "GIT ratio", lines "HeLa"). This is the second reason why the GIT method cannot be directly used as a titration method. Similar result was obtained when using CV-1 cells (data not shown). In addition to human HeLa cells, monkey CV-1 cells and mouse NIH-3T3 cells were infected with the testing and control viruses and GITs, i.e., the transduced number of copies, were measured (lines "HeLa 6.0", "CV-1 6.0" and "NIH-3T3 6.0"). While the GITs of CV-1 and NIH-3T3 cells were 3-fold and 17-fold lower than that